ELSEVIER

Journal of Hazardous Materials A137 (2006) 8–30

Journal of Hazardous Materials

www.elsevier.com/locate/jhazmat

Cellular automata-based forecasting of the impact of accidental fire and toxic dispersion in process industries

Chinmoy Sarkar, S.A. Abbasi *

Center for Pollution Control and Energy Technology, Pondicherry University, Pondicherry 605 014, India

Received 6 December 2004; received in revised form 12 January 2006; accepted 13 January 2006
Available online 19 April 2006

Abstract

The strategies to prevent accidents from occurring in a process industry, or to minimize the harm if an accident does take place, always revolve around forecasting the likely accidents and their impacts. Based on the likely frequency and severity of the accidents, resources are committed towards preventing the accidents. Nearly all techniques of ranking hazardous units, be it the hazard and operability studies, fault tree analysis, hazard indice, etc. – qualitative as well as quantitative – depend essentially on the assessment of the likely frequency and the likely harm accidents in different units may cause. This fact makes it exceedingly important that the forecasting the accidents and their likely impact is done as accurately as possible.

In the present study we introduce a new approach to accident forecasting based on the discrete modeling paradigm of cellular automata. In this treatment an accident is modeled as a self-evolving phenomena, the impact of which is strongly influenced by the size, nature, and position of the environmental components which lie in the vicinity of the accident site. The outward propagation of the mass, energy and momentum from the accident epicenter is modeled as a fast diffusion process occurring in discrete space-time coordinates. The quantum of energy and material that would flow into each discrete space element (cell) due to the accidental release is evaluated and the degree of vulnerability posed to the receptors if present in the cell is measured at the end of each time element. This approach is able to effectively take into account the modifications in the flux of energy and material which occur as a result of the heterogeneous environment prevailing between the accident epicenter and the receptor. Consequently, more realistic accident scenarios are generated than possible with the prevailing techniques. The efficacy of the approach has been illustrated with case studies.

Keywords: Process industry; Accident; Forecasting; Diffusion; Advection; Cellular automata; Modeling

1. Introduction

The science of loss prevention and safety promotion in chemical process industry has witnessed major advancements, especially after the Flixborough and the Seveso disasters which occurred in quick succession during the mid 1970s [1–3]. The R&D in the field were done with even greater sense of urgency and foreboding after the killing and maiming of over 500,000 persons which occurred due to the accidental release of methyl isocyanate at Bhopal in 1984 [3–5].

The provisions of man and material to be made for preventing accidents in a unit of a process industry, and the quantum of monetary resources to be committed for the purpose, are directly related to the risk posed by the unit. And the only rational way to assess the risk is to forecast the accidents likely in the unit and the harm likely to be caused by those accidents. Be it the development of a hazard index [6], a HAZOP (hazard and operability) study [7–9], an MCAA (maximum credible accident analysis) [10], an FTA (fault tree analysis) study [11], or any other exercise in loss prevention and safety implementation, the essential inputs come from the probability and the enormity of the likely accidents.

This fact makes it exceedingly important that accident scenarios are developed as precisely and accurately as possible. Extensive work has indeed been done in this area and the state of the art has been documented in several compendiums, of which the more recent ones include books [3,12] and manuals [13–17] covering several types of accidents. Methodologies for developing scenarios of one or the other specific accident type such as BLEVE (boiling liquid expanding vapour explosion),

* Corresponding author. Tel.: +91 413 2655263; fax: +91 94432 65262.
E-mail address: Prof.S.A.Abbasi@gmail.com (S.A. Abbasi).

0304-3894/$ – see front matter © 2006 Elsevier B.V. All rights reserved.
doi:10.1016/j.jhazmat.2006.01.081

Nomenclature

C	mean air concentration of the toxic pollutant
C_{ijk}	cell toxicity state
${}^{t+1}C_{ijk}$	toxicity state of the cell *ijk* at time *t*
$\Delta^t C^{\text{ad}}_{1-8}$	concentration of toxic material entering the cell *ijk* from each of the eight neighbouring cells in the horizontal plane due to cloud advection
$\Delta^t C^{\text{tur}}_{9-10}$	concentration of toxic material entering the cell *ijk* from the two adjacent cells in the vertical plane due to turbulent diffusion
d	displacement length
D	directionality of the accidental event
E_{ij}	cell energy state
${}^tE_{ij}$	energy state of the cell *ij* at time *t*
${}^{t+1}E_{ij}$	energy state of the cell *ij* at subsequent time $t+1$
$\Delta^2 E_{ij}(t)$	second order difference in the energy of the cell *ij* with respect to the neighbouring cells
g	acceleration due to gravity
H_r	average obstacle height
H_s	heat generation or the release rate divided by the site area
K_x, K_y, K_z	eddy diffusivities along the *x*-, *y*-, and *z*-directions
n	an exponent
${}^t\text{n}_{ij}$, ${}^t\text{s}_{ij}$, ${}^t\text{e}_{ij}$, ${}^t\text{w}_{ij}$, ${}^t\text{ne}_{ij}$, ${}^t\text{nw}_{ij}$, ${}^t\text{se}_{ij}$, ${}^t\text{sw}_{ij}$	directional constants at time *t* associated with the north, south, east, west, northeast, northwest, southeast and southwest directions, respectively
R	cell radius
Ri^*	plume Richardson number
ρ, c_p and T	density, specific heat and temperature of the ambient air
u	mean wind speed
u_T	modified friction velocity
u_*	surface friction velocity
U_x and U_y	mean wind velocities along the *x* and *y* directions
w_e	vertical entrainment velocity
${}^tw_n$, ${}^tw_s$, ${}^tw_e$, ${}^tw_w$, ${}^tw_{ne}$, ${}^tw_{nw}$, ${}^tw_{se}$, and ${}^tw_{sw}$	wind velocity in the north, south, east, west, north-east, north-west, south-east and south-west directions, respectively, at time *t*
z	height
z_0	surface roughness length

Greek letters

α	absorbtivity of the target material present between the accident epicenter and the receptor
β and γ	empirical constants
δ	ground deposition rate of the pollutant
${}^t\delta_{ijk}$	deposition rate of the pollutant in the cell *ijk*
κ	von Karman constant
λ	decay coefficient of the pollutant
${}^t\lambda_{ijk}$	reaction transformation rate of the material in the cell *ijk*
ρ_a	ambient air density
ρ_p	initial density of the flammable gas cloud
τ	atmospheric transmissivity
τ_a	atmospheric transmissivity for adjacent neighbours
τ_b	atmospheric transmissivity for non-adjacent neighbours
ω_a, ω_b	weightage terms for adjacent and non-adjacent neighbours

dust explosion, offshore fires, etc. have also been compiled [18–20].

The common features of the methodologies described in these compendiums and reviews is that for fires and explosion the accidental impact is assumed to be propagating outwards from the accidental epicenter in a radially symmetrical fashion. The only exception is the treatment of jet fire. With this basic assumption, the areas of impact of these accidents are denoted with circles. The areas corresponding to, say, 100%, 50%, 25% probability of death due to an accident are bounded by circles of increasing radii, with the accident site serving as the centre of the circles. In a similar fashion zones of impact are bounded for different probabilities of damage in other manner – for example eardrum rupture, burns, damage to structures, etc. Only when dealing with the accidental jet fire or the release of hazardous gases or liquids the areas of impact are computed on the basis of likely direction of the fire jet or the toxic plume movement. The later, in turn, is predicted on the basis of airshed/watershed characteristics of the accident site, and the 'roughness' of the terrain. But even in these treatments, the aspects such as impact of different types of structures, vegetation, terrain characteristics, etc. are not considered in detail.

The fact is, in real-life situations, the conditions prevailing in the neighbourhood of the accident epicenter are rarely homogeneous. More often than not, the neighbourhood is heterogeneous, comprising of other units, buildings, vegetation, etc. located unsymmetrically with reference to the accident site. The meteorological conditions, especially the wind velocity and direction are also rarely uniform in the vicinity of the accident site. At the instant of time when the accident occurs, this heterogeneity of the neighbourhood strongly influences the outward propagation of not only the mass, but also energy and momentum away from the accident epicentre. Further, due to the heterogeneity of the neighbourhood and the inherently different abilities of the units intercepting the mass/energy/momentum flux, the area-of-impact of an accident would not be radially symmetrical but shall have an irregular shape. Post mortems of major accidents such as the one that occurred in Bhopal [1–4] indicate that entirely different zones of impact would have been created than the one that actually occurred, had the loss of confinement of methyl isocyanate taken place at a different time of the year or at a different hour of the day than it did, or had the topography of the region been different. It follows that a realistic forecast of accidental scenario should take into cognizance the self-evolving nature of

the accident phenomenon, as it is controlled by the heterogeneous conditions prevailing between the accident epicenter and the potential receptor.

In the present study, we propose a cellular automata (CA) based approach for accident modeling in which the spatio-temporal variations in the neighbourhood of the accident site are cognized and accounted for. Two CA based models have been presented which attempt to analyze the dynamics of the propagating flux of energy and toxic material liberated as a result of loss of confinement of a unit. The procedure is based on representing the study area in the form of a grid of 'cells'; the later being squares of preset identical area. The unit suffering an accident is hypothetically placed in one of the cells: the *seed cell*. When the accident occurs, the resultant loss of confinement sends one or more sudden and huge bursts of energy, material and momentum propagating outward and away from the accident epicenter. In the present CA-based treatment, this movement is modeled as occurring from the seed cell (in which the accident epicentre lies) to the adjacent neighbouring cells and then on to the cells lying one after another in the grid, away from the seed cell in all directions. Each cell which intercepts the flux in one direction and exits it in all other directions either reduces the flux or enhances it, depending on the types of objects and the prevailing environmental conditions bounded by the cell. The damage potential of the mass/energy/momentum received in each cell, with reference to a receptor (such as a human being who may get killed or a window-pane which may get shattered), is made the basis for assigning a 'vulnerability level' or a 'vulnerability state' to the cell.

1.1. The accident phenomenon

Chemical process industries are artificial, anthropogenic systems, which process a myriad variety of substances including toxic and flammable materials, and transform them into usable consumer products, often generating byproducts and wastes in the bargain. Such systems have a number of interconnected units with energy and material flowing through them at a controlled rate. In a way, all process units containing energy and/or material in confinement constitute a potential hazard. Any perturbation in the controlled flow through the process units may disrupt the overall equilibrium of the system. If the perturbation is too large to be damped by the safety systems in place, there may be catastrophic build-up of pressure and/or temperature leading to container failure. The resulting loss of confinement may subsequently cause an uncontrolled flow of matter and energy from the unit in to the surroundings. It is this sudden burst of energy as well as, in several cases, release of toxic material that are responsible for the damage caused by the accidents.

The flux of energy or material, which is released by an accident, propagates outwards from the accident epicenter. The

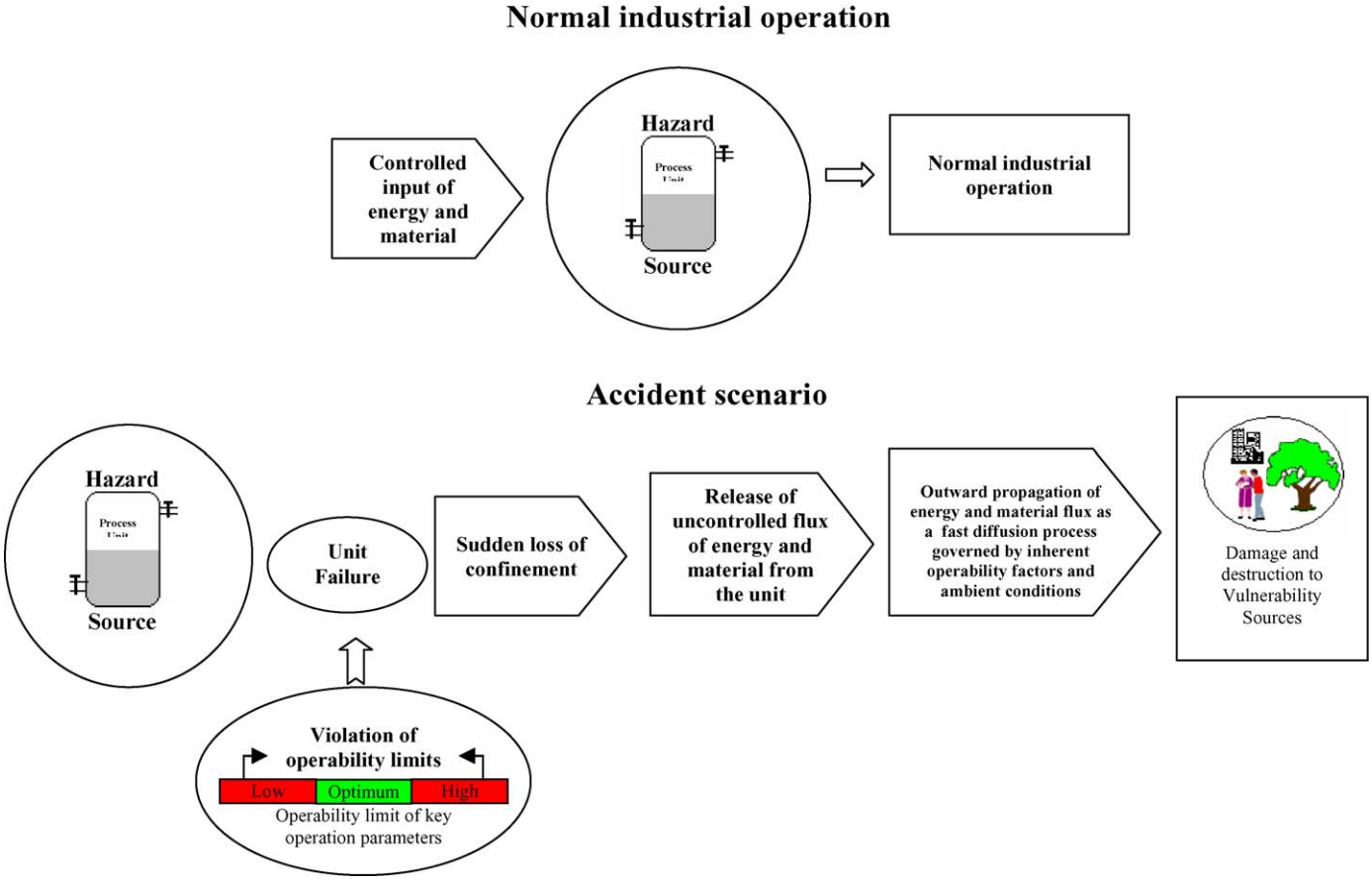

Fig. 1. Conceptual representation of normal industrial operation and an accident situation.

intensity of the flux, and consequently its propensity to cause damage, are governed by:

(a) the enormity of the accident, and
(b) the manner in which the neighbourhood of the accident site attenuates or exacerbates the flux.

Of these 'a' depends upon the nature and the quantity of material being handled, the nature and the degree of wear and stress suffered by the vessel, the extent to which temperature and pressure have exceeded the operable limits, etc.; in other words the 'magnitude of LOC'. The second aspect, 'b', is strongly influenced by the objects and spaces that lie in the path traversed by the flux when it radially propagates away from the accident epicentre. In the case of a thermal flux, the factors which may influence its outward propagation may include the transmissivity and absorptivity of the medium present in its path and the meteorological conditions such as wind speed and direction. The dispersal of toxic chemical will be governed by ambient wind speed and direction, atmospheric stability, the roughness of the terrain, chemical reactions, deposition rates, etc. In other words, an industrial accident may be essentially treated as a *self-evolutionary* phenomenon characterized by the sudden transfer of mass, energy and momentum from a hither to confined space to the surroundings (Fig. 1).

The to-date available risk analysis approaches comprise of techniques to evaluate the magnitude of energy, mass, and momentum exiting an industrial accident but do not cognize the self-evolutionary aspect of the accident. However, any realistic and comprehensive study of an accident and its impact should take cognizance of the underlying mechanisms of the interactive phenomena that define the self-evolution of an accidental scenario. A more comprehensive approach should involve the simulation of the accidental scenarios within the paradigm of a *discrete* model, treating the accident evolution as a fast diffusion process, occurring in discrete space-time coordinates, wherein the outward movement of the flux of energy and material is modified at each time step by the type of objects and other environmental conditions existing at each cell space. Such an approach enables a systematic understanding of interactive subprocesses (following the loss of confinement at the source) that converge on to produce the accident's impact on a given receptor. This conceptual approach for modeling industrial accidents within the framework of cellular automata has been illustrated in Fig. 2.

2. Cellular automata (CA)

In the recent years, cellular automata (CA) has been able to carve out a special niche for itself as a modeling technique capable of mimicking complex, dynamical, self emergent, physical

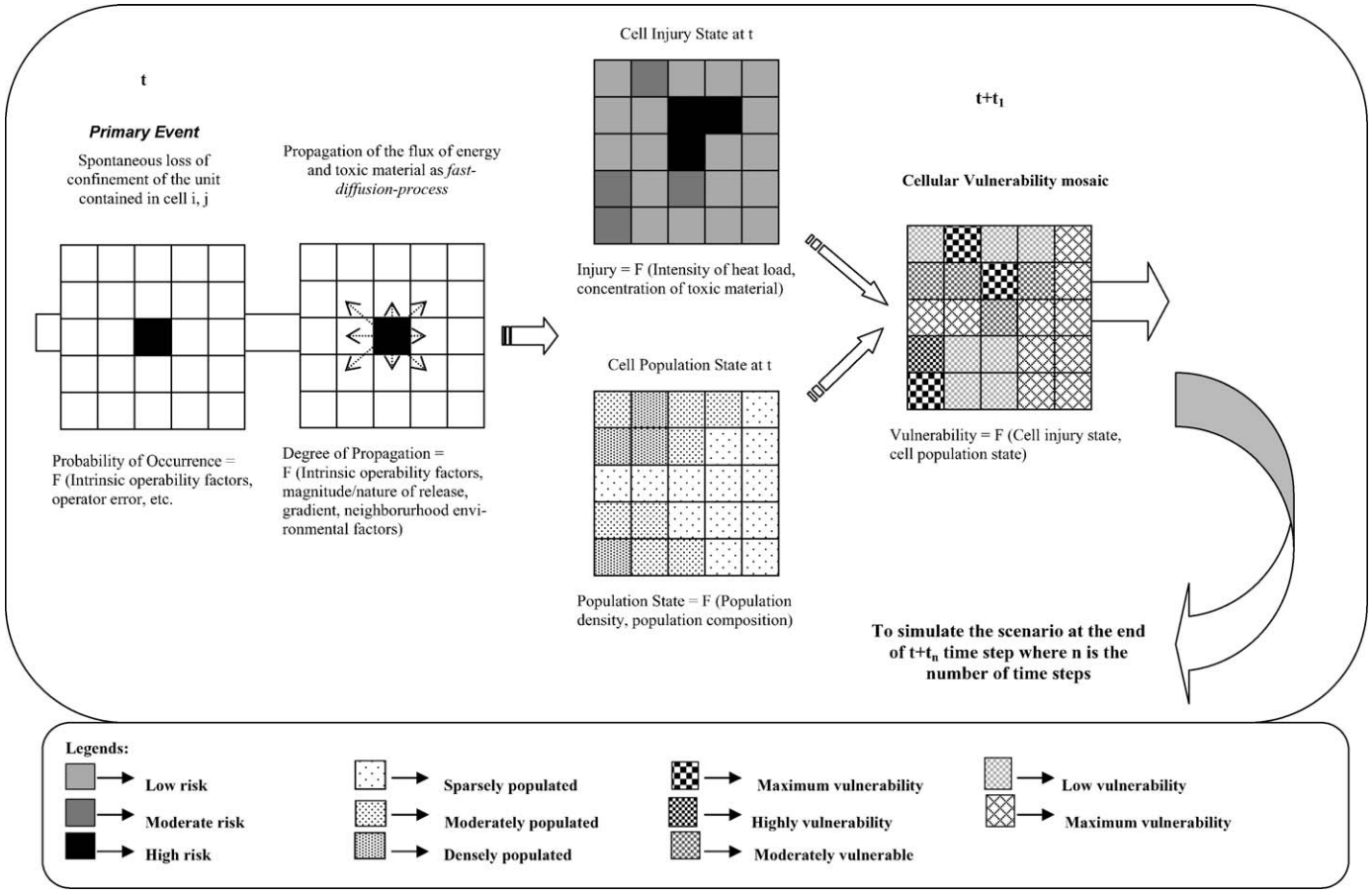

Fig. 2. Cellular automata based approach for modeling the spatio-temporal variations in cellular vulnerability mosaic.

systems comprising of a large number of discrete components with local interactions [21]. The CA approach envisages modeling within the paradigm of discrete space-time coordinates, thereby enabling one to study the 'evolution' or the 'self emergence' of a system at each time step. We believe that accidents occurring in chemical process industry – especially fires and toxic dispersion – are of a nature which makes them amenable to cellular automation. The proposed model is the outcome of this belief. As the propagation of energy liberated from the LOC effects mainly the objects lying along the horizontal axis, it has been treated with two-dimensional CA. On the other hand, the dispersion of toxic gases emanated from the LOC, of which even the ground-level concentration profile is strongly dependant on the three-dimensional dispersion of gaseous plume, has been treated within the framework of a three-dimensional CA.

The term cellular automata has been coined from the words 'cell' and 'automaton'; the former indicates that the space occupied by the system under study is discretized into a lattice of cells, as in a chess board, and the later represents the fact that the state of component cells evolve dynamically according to a set of simple transition rules – the automaton.

The cellular automata theory treats a real life system as if it is composed of an homogeneous lattice of 'cells' in one or multi-dimensional space. The characteristics of the system-component bounded by each cell are described with the help of a unique state assigned to it. The state of each cell in the next time step evolves according to a set of deterministic or probabilistic local transition rules. The transition rules are applied simultaneously on all the cells of the automata, so that their states are synchronously updated in parallel. Consequently, the global state of the system evolves as a result of multiple local level interactions. Cellular automata have also been visualized as a computational tool comprising of a system of parallel processing computers of similar construction.

The conceptual framework of cellular automata was envisioned in the late 1940s as a result of the pioneering work of John von Neumann who was, at that time, also involved in the design of the first digital computer [22]. Neumann conceptualized the development of a machine that would be capable of solving complex problems by imitating the functioning of the human brain and could, at the same time, contain the self-control and self-repair mechanisms with which the human brain is endowed. He was interested in seeking a logical abstraction of the self-reproduction mechanism so evident in many of the life-based processes. With suggestions from Ulam [23], he adopted a fully discrete approach in which space, time, and even the dynamical variables are defined to be discrete. In his abstraction of the problem, Newman actually invented a self-replicating theoretical machine – the first two-dimensional cellular automata [24,25]. It comprised of a square lattice of several thousand elementary cells, each of which could have up to 29 possible states.

However, von Neumann's treatment required far more powerful computational resources than were available at that time and his technique could only be partially implemented on the computers of his era. Indeed, due to the sheer bulk of the computations required in the study of cell matrices, CA was not extensively employed until digital computers became widely available. Subsequently, many others have taken to CA and have been successful in developing many CA rules capable of self-replication using much lesser number of states as the one used by Codd [26], Langton [27], and Byl [28]. In 1970, Conway [24,25] developed the cellular automata based *Game of Life* – an elementary computerized model of a colony of living cells, which became immensely popular following an article published by Gardner [29]. The *Game of Life* is essentially a two-dimensional cellular automaton in which the cells can exist in any of the two possible states: 0, 1. The state of each cell in the subsequent time period is dependant on the status of itself as well as the states of the eight nearest neighbours. The evolution of the system was governed by three transition rules namely survival, death, and birth. Thus, the underlying conceptual ideas of cellular automata were primarily inspired by interactive phenomena often encountered in life science as well as the evolution of the new breed of parallel computational architectures. It is believed that Neumann's enterprising idea of self-reproducing cellular automata had actually anticipated the discovery of the duplicative function of DNA [24]. On account of the striking resemblance between the cellular automaton behavior and many of the physical phenomena, the former has been used as a simulation tool in many branches of study and has gained application in myriad fields of science [30]. It is currently being employed in as diverse fields as architectural design [31], ecology [32–34], epidemiology [35,36], environmental hazard management [37,38], genetics [39], medical sciences [40,41], road traffic flow modeling [42,43], cryptography [44], image processing [45], urban dynamics modeling [46,47] and others, [48].

The ever decreasing cost-capability ratio of computers, ever-enhancing power of parallel computation architecture, and great advancements in the dynamic systems theory – have all led to a renewed surge of interest in cellular automata which has several inherent advantages over conventional mathematical modeling techniques. The main drawback of the conventional techniques – dynamic mathematical models based on differential equations – is that, since in most cases exact quantities are not known, numerical approximations have to be employed. Consequently, these equations may provide information of the overall properties of the physical systems, but cannot account for the individual components of the system [49,50]. For example, the study of temporal evolution of a system from an initial state q_0 to the state q_t in t time steps using a partial differential equation approach entails constructing one by one each of the intermediate steps $q_0, \ldots, q_t$ and subsequently performing numerical integration. In contrast, on account of the inherent discreteness of the cellular automata (CA) models, the numerical integration in CA is a more exact process, wherein there is no truncation or round-off of errors to worry about. Consequently, CA provides a more accurate description of each individual components of the system under study. Yet another potential superiority of this class of models emerges from the fact that, in contrast to the equation driven approach envisaged by the conventional models, they are able to delve much deeper into the transient, underlying, mechanisms of interactions governing the self evolution of a system [51]. As a result, there is explicit correspondence between the physical and computational processes. A concep-

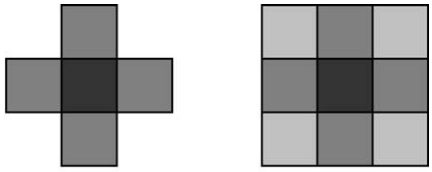

Fig. 3. Neighbourhoods in a CA Model – Von Neumann Neighbourhood (a) and Moore Neighbourhood (b). The shades indicate the different orientation of the neighbours with respect to the central cell.

tually clearer, more accurate and comprehensive understanding of the system is achieved. Further, due to the inherent parallelism of the CA-based models, they can fit into the parallel computational architecture, enabling complex simulations to be performed within very short periods.

According to Itami [25], CA is defined by:

$$Q = \langle S, N, T \rangle \tag{1}$$

where Q is the global state of the system, S a set of all possible states of the cellular automaton, N a neighbourhood of all cells that provides input values for the transition function T, and T is a transition function that defines the change in the state of the cellular automaton from its state in time t to the state in the next time step $(t+1)$.

Five essential elements form the building blocks of any CA model:

1. *Cell space*: refers to the space occupied by the system under study in which the simulation process operates. It may be a lattice of cells in two-dimensional space in the case of 2D CA. The cell space of a 3D CA consists of a lattice of cubical cells in three dimensions. A fundamental characteristic of the lattice is that the cells have some adjacency or proximity to one another in the same way as land parcels do in urban systems. Usually the lattice is a uniform grided space and, theoretically, the cells may be of any geometric shape.
2. *Cell states*: refers to any one state of a set of possible states defined by the system being modeled, that each cell in the lattice can adopt at a time.
3. *Time steps*: refer to the discrete time interval at which the evolution of the cell system is studied. At the end of each time step, the state of each cell within the system is updated on the basis of predefined transition rules.
4. *Neighbourhood*: of a cell envelops the other cells that lie adjacent to it. The state of a cell is influenced by the configuration of its neighbourhood. In two-dimensional CAs, the neighbourhood is usually four or eight nearest neighbours. The neighbourhood consisting of the central cell and its four nearest neighbours is often called the von Neumann neighbourhood while the next nearest neighbours comprising of eight cells surrounding the central cell is referred as Moore neighbourhood (Fig. 3). In a three dimensional cellular automata, the neighbourhood comprises of 26 cells surrounding the central cell.
5. *Transition rules*: are the mathematical functions which govern the nature of transformation of the cell states in a cellular automata. These rules are based on the forcing factors that govern the cell transition and are employed synchronously on all the cells of the lattice. In other words, these rules govern the dynamic evolution of the state of the system as a whole so that a new state with a different set of configuration is generated at the end of each time step. Thus, the transition rules govern the nature of transition in the each of the cell states of the system in the subsequent time interval which in turn depend on the current state of a cell as well as its neighbourhood configuration.

It follows that an n-dimensional cellular automaton is composed of a matrix of identical cells regularly arranged in n dimensions. At any given instant of time, each cell can take up a single value, or a state, out of a set of possible values or states. In the simplest case the state is either zero or one. The lattice of cell states at time zero $(t=0)$ is referred to as the initial state. In subsequent time steps $(t+1, t+2, t+3, \ldots, t+n)$, the state of all cells in the lattice changes as a function of the cell's current state as well as the state of the local or the neighbouring cells. Often the function is expressed by summing the values of the neighbouring cells and applying a deterministic rule, based on the value of the cell's current state, and the neighbourhood sum. This function is applied to the entire lattice of cells synchronously, i.e. in the same time step. The resulting configuration of cell values defines the state of the system in the next time step $(t+1)$. In computing terms, this is referred to as a recursive algorithm. Thus the state of a cell at time $(t+1)$ can be represented as the function of its state at time t, its neighbourhood, and the transition rule, and it is given by:

$$S_{t+1} = f(S_t, N, T) \tag{2}$$

where S_{t+1} is the state of a cell at time $(t+1)$, S_t the state of the cell at time t, N the neighbourhood, and T is a set of transition rules governing the cells.

The predictive capacity of the CA based decision models depends upon the accuracy of the transition rules. Several methods exist for setting the transition rules in the CA models; which are being continuously advanced and fine-tuned. Quantitative mathematical techniques such as artificial neural networks [52,53], genetic algorithm [54,55], Markov chains [56], Monte Carlo simulation [57,58], fuzzy logic [59,60], and multi-criteria evaluation techniques [61] have been used for the development of CA-based transition rules.

3. Modeling the propagation of energy liberated at the accident epicentre

During accidents, the dominant form of energy that causes maximum damage is the thermal energy which propagates via conduction, convection, and radiation. In most cases, it is the thermal *radiation* that constitutes maximum hazard. In forecasting the impact of accidental bursts of energy, the role of the participating medium in diluting or augmenting the energy flux needs to be carefully understood. Unlike in absolute vacuum, the participating media may attenuate the released radiation photons

due to absorption and scattering. For example, if an obstacle happens to lie in the path of the energy flux, it would modify the pattern of energy propagation by absorbing a part of the incoming flux. When appreciable heat conduction and/or convection occur simultaneously with radiation in an *absorbing-emitting medium*, the mathematics associated with its treatment becomes exceedingly complex. But, the treatment can be simplified without significant loss of accuracy by modeling the phenomenon as a *fast diffusion process.* Incase of an optically dense and heterogeneous medium, like the one encountered in real-life situations, absorption and scattering would cause the radiative energy flux to travel a shorter distance compared to the distance it may travel in vacuum. Consequently, the penetration distance of the radiant energy flux is smaller compared to the distance over which significant temperature changes occur. In such conditions, it is possible to transform the integral type equations that result from radiative energy balance into a diffusion equation [62]. This equation is analogous to the heat transfer equation where the propagation of energy can be described in terms of the gradient of the conditions in the immediate vicinity of the accident epicenter. The application of this diffusion approximation produces great simplification in treating the problems of radiative transfer during accidents, especially industrial fires.

The phenomenon of diffusion occurring in an isotropic medium may be expressed by the following equation:

$$\frac{\delta P}{\delta t} = \frac{\delta}{\delta x}\left(\rho \frac{\delta P}{\delta x}\right) + \frac{\delta}{\delta y}\left(\rho \frac{\delta P}{\delta y}\right) + \frac{\delta}{\delta z}\left(\rho \frac{\delta P}{\delta z}\right) \tag{3}$$

where $(\delta P/\delta t)$ is the rate of transfer per unit space, P the concentration of the diffusing substance, and ρ is the diffusion coefficient which measures the transmissivity or the conductance of the medium. When solved numerically, Eq. (3) takes the form:

$$P_{ij}(t + \Delta t) = P_{ij}(t) + \rho \nabla^2 P_{ij}(t)\Delta t \tag{4}$$

where i and j are the row and column numbers, respectively, defining the special location of the cell and ∇^2 is the Laplacian operator. In two-dimensional coordinates, the above equation may be modified as

$$P_{ij}(t + \Delta t) = P_{ij}(t) + \rho \Delta^2 P_{ij}(t)\Delta t \tag{5a}$$

where $\Delta^2 P_{ij}(t)$ is the second order difference. Since we are considering the fast diffusion of the radiation flux liberated from the accident epicenter, the above equation may be re-written as:

$$E_{ij}(t + \Delta t) = E_{ij}(t) + \rho \Delta^2 E_{ij}(t)\Delta t \tag{5b}$$

where $E_{ij}(t)$ is the density of the energy flux reaching the cell ij at the end of time t, and $\Delta^2 E_{ij}(t)$ is the second order difference term originating as a result of diffusion from the neighbouring cells.

3.1. A CA-based approach for simulating energy propagation during accidental scenarios

We have developed a cellular automata model for the accident scenario generation in case of loss of confinement and the subsequent uncontrolled flow of energy. The consequence assessment is performed by evaluating the vulnerability of the cells associated with the space through which the uncontrolled flux of energy propagates after an LOC. In the proposed model, the cellular vulnerability has been deemed to be a function of three factors, namely

1. *Cell energy state* (E_{ij}): This reflects the quantum of unbalanced energy reaching a cell at a time t as a result of LOC and subsequent uncontrolled flow of energy into the surroundings.
2. *Cell population state* (P_{ij}): This indicates the magnitude and characteristics of vulnerable population present in a given cell ij at time t. Accurate assessment of the composition and density of the receptor population are essential for accurate impact prediction.
3. *Cell injury state* (In_{ij}): It is a function of the cell *energy* state. The cell injury state evaluates the potential of the uncontrolled energy released as a result of LOC of a unit to cause injury or damage.

Hence, the vulnerability of a cell ij in terms of the magnitude of injury posed to the human populations due to the uncontrolled flux of energy liberated as a result of LOC of a unit may be expressed as

$$^{t+1}V_{ij} = f(E_{ij}, P_{ij}, \mathrm{In}_{ij}) \tag{6}$$

3.1.1. Cell energy state

We have hypothetically divided the study area into a lattice of cells. In presence of a heterogeneous absorbing medium comprising of the atmosphere and various objects, the dynamics of propagation of the liberated thermal radiation has been studied as a fast diffusion process. This implies that energy flux liberated from the accident epicentre travels outwards to the adjoining cells and once each of these incident cells become saturated with energy, they in turn begin to act as energy sources and the flux begins to diffuse from these cells into their respective neighbourhoods. Thus the driving forces governing this outward propagation of the energy flux are the magnitude of the energy gradient existing among the cells as well as the characteristics of the space enveloped by these cells. In a nutshell, the energy state of any cell ij in the time $t+1$ will be a function of its energy state in the preceding time t, the magnitude of energy gradient with respect to neighbouring cells, the prevailing atmospheric transmissivity in the cell, degree of absorbtivity of any intercepting object localized in the cell as well as the directionality of the event. The energy state of any cell ij in time $t+1$ may hence be represented as

$$^{t+1}E_{ij} = f(^{t}E_{ij}, \Delta^{t}E_{1-8}, \tau, \alpha, D) \tag{7}$$

where $^{t}E_{ij}$ represents the energy state of the cell ij at time t, $\Delta^{t}E_{1-8}$ represents the magnitude of positive energy gradient with respect to each of the eight neighbouring cells, τ the atmospheric transmissivity, α is the absorbtivity of the target material. The directionality of the event is represented by D.

3.1.1.1. Attenuation by the atmosphere. Significant attenuation of energy occurs as the flux passes through atmospheric space between the source and the receptor. But quantifying the degree of attenuation thus possible is fraught with uncertainty as the atmospheric conditions may vary sharply in time as well as in space. Furthermore, energy of varying frequency would meet with varying degrees of attenuation.

The energy received by a given cell would depend upon two factors:

- the orientation of the neighbouring cell, i.e. the location of the neighbouring cell with reference to the cell being studied;
- prevalent atmospheric conditions, especially the existence of absorbing gases like CO_2 and water vapour.

The following expression for the atmospheric transmissivity has been proposed [63]

$$\tau = 2.02(P_{\mathrm{w}}a)^{-0.09} \tag{8}$$

We have employed a slightly modified version of the above expression by incorporating a weightage term to evaluate the transmissivity along the adjacent and non-adjacent neighbours. Thus, for the adjacent neighbours

$$\tau_{i-1,j} = \tau_{i+1,j} = \tau_{i,j-1} = \tau_{i,j+1} = \tau_{\mathrm{a}} \tag{9}$$

and for the non-adjacent neighbours

$$\tau_{i-1,j-1} = \tau_{i-1,j+1} = \tau_{i+1,j-1} = \tau_{i+1,j+1} = \tau_{\mathrm{b}} \tag{10}$$

in the above expressions,

$$\tau_{\mathrm{a}} = 2.02(P_{\mathrm{w}})^{-0.09}\omega_{\mathrm{a}} \qquad \tau_{\mathrm{b}} = 2.02(P_{\mathrm{w}})^{-0.09}\omega_{\mathrm{b}}$$

$$\omega_{\mathrm{a}} > \omega_{\mathrm{b}}; \omega_{\mathrm{a}} + \omega_{\mathrm{b}} = 1$$

$$P_{\mathrm{w}} = 1013.25(\mathrm{RH})\ \exp\left(14.4144 - \frac{5328}{T_{\mathrm{a}}}\right)$$

where a is the length of the side of the cells, T_{a} the ambient temperature in K and RH is the relative humidity. The weightage term for the adjacent neighbours has been taken as 0.88 while for non-adjacent neighbours, it has been taken as 0.18.

3.1.1.2. Cell neighbourhood. We have used the 'Moore neighbourhood' which comprises of eight immediate neighbours to each cell. There are two types of neighbours depending upon their orientation around the central cell – the adjacent neighbours and the non-adjacent neighbours. The amount of energy that is allocated to a given cell depends upon the extent of energy gradient existing between the cell and its neighbours. The energy flux in a cell ij at the time step $t+1$ would depend on the magnitude of the energy present in the cell at the time t as well as the amount of energy that has diffused from the neighbouring cells (as indicated by Eq. (5b)). Thus,

$${}^{t+1}E_{ij} = {}^{t}E_{ij} + \tau\Delta^2 E_{ij}(t) \tag{11}$$

The quantum of energy that has diffused from the neighbouring cells may be obtained from the following expression:

$$\begin{aligned}\tau\Delta^2 E_{ij}(t) = {} & \tau_{\mathrm{a}}[(E_{i-1,j} - E_{ij}) + (E_{i+1,j} - E_{ij}) \\ & + (E_{i,j+1} - E_{ij}) + (E_{i,j-1} - E_{ij})] \\ & + \tau_{\mathrm{b}}[(E_{i-1,j-1} - E_{ij}) + (E_{i-1,j+1} - E_{ij}) \\ & + (E_{i+1,j-1} - E_{ij}) + (E_{i+1,j+1} - E_{ij})]\end{aligned} \tag{12}$$

Therefore,

$$\begin{aligned}{}^{t+1}E_{ij} = {} & {}^{t}E_{ij} + \tau_{\mathrm{a}}[(E_{i-1,j} - E_{ij}) + (E_{i+1,j} - E_{ij}) \\ & + (E_{i,j+1} - E_{ij}) + (E_{i,j-1} - E_{ij})] \\ & + \tau_{\mathrm{b}}[(E_{i-1,j-1} - E_{ij}) + (E_{i-1,j+1} - E_{ij}) \\ & + (E_{i+1,j-1} - E_{ij}) + (E_{i+1,j+1} - E_{ij})] \\ \forall E_{i-1,j} > {} & E_{ij}; E_{i+1,j} > E_{ij}; E_{i,j+1} > E_{ij}; E_{i,j-1} \\ & > E_{ij}; E_{i-1,j-1} > E_{ij}; E_{i-1,j+1} > E_{ij}; E_{i+1,j-1} \\ & > E_{ij}; E_{i+1,j+1} > E_{ij}\end{aligned} \tag{13}$$

The above condition refers to the sequential, unidirectional, diffusion occurring only along the positive gradient.

3.1.1.3. Time steps. The overall dynamics of the system undergoing an accident varies with time vis a vis variations in the flux of energy and matter liberated due to the LOC. The events are assumed to occur in discrete time steps. If the LOC takes place at time t, the impact scenarios may be generated for the subsequent time steps $t+1, t+2, t+3, \ldots, t+n$.

3.1.1.4. Direction of the mass/energy flux. Based on the nature of the LOC caused by an accident the initial flow of mass/energy may be greater in some directions than other. This 'directionality' of LOC depends upon the nature and the position of the unit suffering LOC as well as the prevailing ambient conditions:

$$\begin{aligned}\text{Directionality} = {} & f(\text{physico} - \text{chemical properties of the} \\ & \text{material being handled, operating} \\ & \text{conditions, mechanical properties of the} \\ & \text{tank, prevailing ambient conditions})\end{aligned} \tag{14}$$

The 'directionality' of the event will play an important role in determining the pattern of energy propagation from the unit. Assuming that there is a pool fire and also further assuming that there is a strong wind current oriented from north to south, it follows that the amount of energy diffusing into the cell ij from the northern neighbour ij would be much more while the amount of energy diffusing into the cell ij from its southern neighbour would be considerably lesser as compared to the condition prevailing in absence of any wind currents. In order to incorporate this directionality factor into the model, eight directional constants ${}^{t}\mathrm{d}_{ij}$, i.e. ${}^{t}\mathrm{n}_{ij}$, ${}^{t}\mathrm{s}_{ij}$, ${}^{t}\mathrm{e}_{ij}$, ${}^{t}w_{ij}$, ${}^{t}\mathrm{ne}_{ij}$, ${}^{t}\mathrm{nw}_{ij}$, ${}^{t}\mathrm{se}_{ij}$, ${}^{t}\mathrm{sw}_{ij}$ have been assigned to the neighbourhood cells located in the north, south, east, west, northeast, northwest, southeast and southwest directions respectively. The effect of this factor upon the energy

allocation in any cell in the CA matrix diminishes with increasing distance of the cell from the 'seed cell' – i.e. the cell where the loss of confinement had occurred. Thus, the magnitude of the directionality factor may be expressed as:

$$D = 1 + \left(\frac{1}{r^n}\right) {}^{t}d_{ij} \tag{15}$$

where r is the cell radius considered from the cell where the LOC has taken place, n is an exponent and ${}^{t}d_{ij}$ is the directional constant associated with the specific direction. The numerical values assigned to these directional constants are calibrated according to the importance and degree of the directionality of the event. In this example we have assigned to the exponent the value 1 for simplicity.

If the flux of energy from an LOC happens to be oriented along the direction from X to Y, then the directional constant associated along the positive X-direction is assigned a negative value, i.e. $(1 + {}^{t}X_{ij}) < 1$ to account for lesser diffusion of energy in that direction. On the other hand, the directional constant associated with the positive Y-direction would have a positive value ie $(1 + {}^{t}Y_{ij}) > 1$ due to considerably greater diffusion along the Y-direction as compared to the situation prevailing in absence of any directionality factor.

$$\begin{aligned}
{}^{t+1}E_{ij} = {}^{t}E_{ij} + \tau_{\mathrm{a}} \Bigg[& \left(1 + \frac{{}^{t}\mathrm{n}_{ij}}{r}\right)(E_{i,j+1} - E_{ij}) \\
& + \left(1 + \frac{{}^{t}\mathrm{e}_{ij}}{r}\right)(E_{i+1,j} - E_{ij}) + \left(1 + \frac{{}^{t}\mathrm{s}_{ij}}{r}\right) \\
& \times (E_{i,j-1} - E_{ij}) + \left(1 + \frac{{}^{t}\mathrm{w}_{ij}}{r}\right)(E_{i-1,j} - E_{ij})\Bigg] \\
& + \tau_{b} \Bigg[\left(1 + \frac{{}^{t}\mathrm{ne}_{ij}}{r}\right)(E_{i-1,j+1} - E_{ij}) + \left(1 + \frac{{}^{t}\mathrm{nw}_{ij}}{r}\right) \\
& \times (E_{i-1,j-1} - E_{ij}) + \left(1 + \frac{{}^{t}\mathrm{se}_{ij}}{r}\right)(E_{i+1,j+1} - E_{ij}) \\
& + \left(1 + \frac{{}^{t}\mathrm{sw}_{ij}}{r}\right)(E_{i+1,j-1} - E_{ij})\Bigg]
\end{aligned} \tag{16}$$

To illustrate the concept it may be said that if the directionality of an event is from east to west, then the values of the directional constants in the above equation will have the following relationships:

$$\begin{aligned}
& {}^{t}\mathrm{w}_{ij} > {}^{t}\mathrm{nw}_{ij} = {}^{t}\mathrm{sw}_{ij} > 0 \qquad {}^{t}\mathrm{n}_{ij} = {}^{t}\mathrm{s}_{ij} = 0 \\
& {}^{t}\mathrm{e}_{ij} < {}^{t}\mathrm{ne}_{ij} = {}^{t}\mathrm{se}_{ij} < 0
\end{aligned} \tag{17}$$

3.1.1.5. Absorption. If any object happens to lie in the path of the energy flux emanating from the accident epicentre, the object would absorb a fraction of the incident energy, resulting in a discernable attenuation of the flux. In the CA-based model under discussion, the energy flux has been conceptualized as moving through a grid of cells. One or more of the cells may contain objects which may absorb or deflect, thereby attenuating the energy flux. As an example, we assume that during its outward propagation from the accident epicentre to the receptor, the flux has to travel through cells containing concrete buildings, vegetation canopy and a water body; each of the objects will absorb fractions of the incident energy to varying degree depending upon their absorbtivities so that the amount of energy that will actually reach the receptor would be considerably lesser than if there were no intercepting objects. Another likelihood is that the energy flux may have to pass through cells containing another hazardous unit. In such a situation, there always exists the probability that the intercepting unit may absorb sufficient energy so as to suffer an LOC in the subsequent time step; in other words a second accident may be caused by the initiating event, thereby contributing to the energy flux of the initiating event. It follows that, the nature of the objects present in the path of the propagating energy flux and their absorbtivity is a very important factor which governs the *self evolution* of any accident scenario. This factor can be incorporated into the energy function by introducing the constant α, which is the absorbtivity of the object occupying a cell. The net unbalanced energy in any cell ij at time $t+1$ may be expressed as:

$$\begin{aligned}
{}^{t+1}E_{ij} = {}^{t}E_{ij} + \tau_{\mathrm{a}}(1-\alpha) \Bigg[& \left(1 + \frac{{}^{t}\mathrm{n}_{ij}}{r}\right)(E_{i,j+1} - E_{ij}) \\
& + \left(1 + \frac{{}^{t}\mathrm{e}_{ij}}{r}\right)(E_{i+1,j} - E_{ij}) + \left(1 + \frac{{}^{t}\mathrm{s}_{ij}}{r}\right) \\
& \times (E_{i,j-1} - E_{ij}) + \left(1 + \frac{{}^{t}\mathrm{w}_{ij}}{r}\right)(E_{i-1,j} - E_{ij})\Bigg] \\
& + \tau_{\mathrm{b}}(1-\alpha) \Bigg[\left(1 + \frac{{}^{t}\mathrm{ne}_{ij}}{r}\right)(E_{i-1,j+1} - E_{ij}) \\
& + \left(1 + \frac{{}^{t}\mathrm{nw}_{ij}}{r}\right)(E_{i-1,j-1} - E_{ij}) + \left(1 + \frac{{}^{t}\mathrm{se}_{ij}}{r}\right) \\
& \times (E_{i+1,j+1} - E_{ij}) + \left(1 + \frac{{}^{t}\mathrm{sw}_{ij}}{r}\right) \\
& \times (E_{i+1,j-1} - E_{ij})\Bigg]
\end{aligned} \tag{18}$$

3.1.2. Cell population state

In the proposed model, the cell population state P_{ij} has been expressed in terms of the total population density residing in the cell ij at time t.

3.1.3. Cell injury state

The cell injury state evaluates the potential of the flux of energy, released due to LOC, to cause injury. The most commonly employed approach is to express the likelihood of the injury (including fatal injury) in terms of probit function. The later relates the percentage of people likely to be injured upto a defined extent (say first degree burns/third degree burns/death) in a bounded region to the magnitude of a particular accident event through a log-normal distribution function. The probit equations for some hazards were first given by Lees [2] and since then this approach continues to be employed in the damage effect calculations for different accident scenarios [13,64–66].

The probit function for fatal burn injuries have been expressed as [2]:

$$Y = -14.9 + 2.56 \ln (tI^{4/3} \times 10^{-4}) \quad (19)$$

where I is the intensity of thermal radiation (W/m^2), t the time of exposure, and Y is the probit value.

In the model proposed by us, the injury state of a cell ij evaluates the percentage probability of damage p_{ij} for the cell. It is a function of the magnitude of energy flux allocated to the cell as well as the length of the time step (which reflects the duration of exposure). It may be expressed as:

$$^{t+1}\mathrm{In}_{E_{ij}} = {}^{t+1}p_{E_{ij}} = f({}^{t+1}\Phi_{E_{ij}}, \Delta t) \quad (20)$$

where $p_{E_{ij}}$ is the probability of damage due to energy flux $^{t+1}\Phi_{E_{ij}}$ reaching the cell ij at time $t+1$ and Δt is the length of each time step.

Thus, the overall cell vulnerability state of the cell ij with respect to the energy released due to the LOC in time $t+1$ – $^{t+1}V_{ij}$ – may be expressed as:

$$^{t+1}V_{ij} = ({}^{t+1}P_{ij} \times {}^{t+1}p_{Eij}) \quad (21)$$

4. Dispersion of toxic gases

During the emission of toxic gases after the LOC of a unit and the formation of a cloud, the initial morphology of the toxic cloud is governed by the internal cloud buoyancy effects. The neutrally or positively buoyant gases tend to leave the ground surface and become mixed with the prevailing ambient air flow. On the contrary, in the case of dense gases, gravity currents are set up in the initial phase and they drive the initial flow within the cloud, more or less independent of the mean wind speed. In this phase, the gravity front at the edge of the cloud induces mixing.

Thereafter, the transportation of the toxic materials in the atmosphere is governed by the following processes:

- *Advection*: Advective transport is the movement of the pollutant particles entrained in a current. The effective transport speed, U_e, also termed as the cloud advective speed, is dependant upon the time-varying three-dimensional wind field. The prevailing wind direction plays a very important role: the maximum impact of a toxic release is experienced downwind. Nevertheless, dense gases tend to spread laterally, and, possibly, upwind. Greater the wind speed more is the rate of dilution.
- *Turbulent diffusion*: Turbulent or eddy diffusion refers to the mixing of the pollutant particles as a result of the macroscopic turbulence which arises due to eddies in the turbulent shear flow. It may be measured by the rate of spread of the pollutant cloud (in the vertical, lateral or downwind directions) about its center of mass. The eddy diffusivity can be several orders of magnitude larger than the molecular diffusivity.The phenomenon of turbulent diffusion depends upon several factors such as the surface roughness conditions, wind speed, stability conditions, gas density, etc. Mechanical turbulence arises as a result of the variations of the wind speed and surface roughness elements and causes a sort of mixing or stirring of the air. The presence of intercepting objects – buildings and other obstacles on the ground – causes a distortion in the atmospheric boundary layer flow, thereby influencing the dispersion of the toxic cloud. In a majority of the cases, there is a decrease in concentration from low level releases, although increased concentrations may also be observed. The presence of an obstacle results in increased height and width of the cloud, and increased residence times, thereby posing enhanced risk to the ground level receptors. The effect is more evident in the cases of dense gas clouds. Buoyant turbulence is generated by the heating of the ground surface by the sun and is suppressed by the cooling of the ground at night. Thermal sources within the obstacle array, such as the energy stored in buildings and industrial plants in an urban system, may also cause turbulence.The action of atmospheric turbulence is more efficient under unstable conditions whereas the turbulent mixing is reduced in a strongly stable atmosphere.
- *Chemical reaction rate*: Chemical reactions may convert the initially released toxic material into a secondary pollutant. The rate of decay is indicated by the decay coefficient that governs the transformation of the primary material released.
- *Deposition rate*: The toxic material released as a result of LOC of a unit may be removed from the cloud through the deposition of the material on the ground. This may be accompanied by one or more of the mechanisms: dry deposition of gases on the surfaces, and wet deposition by precipitation of the gases from the cloud.

The advection–diffusion equation governing the dispersion of a pollutant cloud may be written as follows:

$$\frac{\partial C}{\partial t} = \underbrace{\frac{\partial}{\partial x}\left(K_x \frac{\partial C}{\partial x}\right) + \frac{\partial}{\partial y}\left(K_y \frac{\partial C}{\partial y}\right) + \frac{\partial}{\partial z}\left(K_z \frac{\partial C}{\partial z}\right)}_{\text{Turbulent diffusion component}} \underbrace{- U_x \frac{\partial C}{\partial x} - U_y \frac{\partial C}{\partial y}}_{\text{Advection component}} \underbrace{- \delta C}_{\text{Chemical transformation component}} \underbrace{\pm \lambda C}_{\text{Deposition component}} \quad (22)$$

where C is the mean air concentration of the toxic pollutant species, U_x and U_y the mean wind velocity components along the x and y directions, t the time, K_x, K_y and K_z the eddy diffusivities along the three coordinate directions, δ the ground deposition rate of the pollutant, and λ is the decay coefficient of the pollutant. The above equation may be generalized as:

$$\frac{\partial C}{\partial t} = \sum_{i=x,y,z} \left[K_i \frac{\partial^2 C}{\partial i^2} - U_i \frac{\partial C}{\partial i} - \delta C \pm \lambda C \right] \quad (23)$$

where i represents the coordinates in which the processes are considered.

4.1. A CA-based approach for simulating dispersion of accidentally released toxic gases

We propose a model based on three-dimensional CA to simulate the atmospheric dispersion of toxic gas cloud emanating as a result of LOC of a unit. The model takes into account the key governing factors – the extent of cloud advection, turbulent diffusion, deposition of the material contained in the toxic cloud, and the transformation rate of the toxic material – and evaluates the cell vulnerability. The cell vulnerability has been considered to be a function of three states namely:

1. *Cell toxicity state* (C_{ijk}): It gives an indication of the toxicity levels prevailing in the cell in terms of the concentration of the toxic material.
2. *Cell population state* (P_{ijk}): It indicates the magnitude and characteristics of vulnerable population present in the cell *ijk*.
3. *Cell injury state* (In_{ijk}): As defined earlier in the case of energy propagation model, the cell injury state is a function of the cell toxicity state. The cell injury state evaluates the injury or damage caused by the toxic material released as a result of LOC of a unit.

4.1.1. Cell toxicity state

The study area has been represented as a three dimensional lattice of cubical cells. During the LOC of a process unit and the subsequent release of toxic materials, the concentration of the toxic material in any arbitrary cell *ijk* depends upon the extent of dilution and dispersion characteristics of the toxic cloud. For the sake of simplicity we have considered the impact of cloud advection along the horizontal direction, while the effect of turbulent diffusion has been considered only along the vertical plane. The cell neighbourhood is thus defined by ten surrounding cells – eight immediate neighbours in the horizontal plane which consists of four adjacent neighbours and four non-adjacent neighbours, and two immediate neighbours in the vertical plane, as shown in Fig. 4. The flux of toxic concentration emanating from the eight neighbouring cells in the horizontal plane to the cell *ijk* is governed by the cloud advective speed, while the flux emanating from the two adjacent neighbours in the vertical plane is governed by the extent of turbulent diffusion. Two types of weighing parameters have been employed for the two categories of neighbours as given below:

For adjacent neighbours:

$$\omega_{i,j,k-1} = \omega_{i-1,j,k} = \omega_{i+1,j,k} = \omega_{i,j+1,k} = \omega_{i,j-1,k} = \omega_{i,j,k+1} = \omega_{\mathrm{a}}$$

For the non-adjacent neighbours:

$$\omega_{i+1,j-1,k} = \omega_{i-1,j-1,k} = \omega_{i+1,j+1,k} = \omega_{i-1,j+1,k} = \omega_{\mathrm{b}}$$

Thus, in discretized terms, the cell toxicity state of a cell *ijk* in the time $t+1$ may be defined as:

$$^{t+1}C_{ijk} = f(^{t}C_{ijk}, \Delta^{t}C^{\mathrm{ad}}_{1-8}, \Delta^{t}C^{\mathrm{tur}}_{9-10}, {}^{t}\delta_{ijk}, {}^{t}\lambda_{ijk}) \quad (24)$$

where $^{t}C_{ijk}$ represents the toxicity state of the cell *ijk* at time t, $\Delta^{t}C^{\mathrm{ad}}_{1-8}$ represents the concentration of toxic material entering the cell *ijk* from each of the eight neighbouring cells in the horizontal plane due to cloud advection, $\Delta^{t}C^{\mathrm{tur}}_{9-10}$ is the concentration of toxic material entering the cell *ijk* from the two adjacent neighbours in the vertical plane as a result of atmospheric turbulent diffusion, $^{t}\delta_{ijk}$ denotes the deposition rate of the material in the cell *ijk* and $^{t}\lambda_{ijk}$ symbolizes the decay coefficient or the transformation rate of the material in the cell *ijk*.

4.1.1.1. Advective transport. Advective transport of the toxic cloud is governed by the prevailing wind speed and direction, and results in the dilution of the pollutant concentration. In the present study, the cloud advection due to the prevailing wind field is considered along the horizontal plane. The concentration of the pollutant in a cell *ijk* in the subsequent time interval $t+1$ depends upon the magnitude of the concentration in the cell at the time t ($^{t}C_{ijk}$) as well as the amount entrained from the eight immediate neighbours in the horizontal plane ($\Delta^{t}C^{\mathrm{ad}}_{1-8}$). The second factor depends upon the magnitude of the prevailing wind speed along the eight directions. Thus, the pollutant

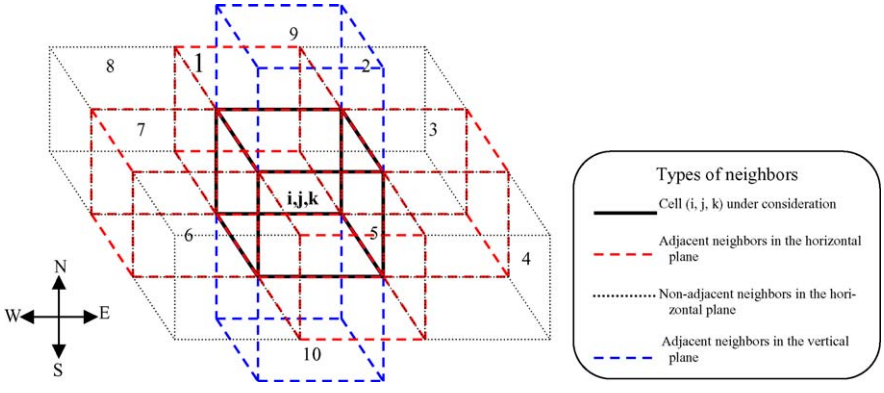

Fig. 4. A cellular automaton comprising of a lattice of cubical cells with ten cell neighbourhood – six adjacent neighbours and four non-adjacent neighbours.

concentration in the cell *ijk* at time $t+1$ may be expressed as:

$$
\begin{aligned}
{}^{t+1}C_{ijk} = {} & \omega_{\mathrm{a}}[{}^{t}w_{\mathrm{n}}(C_{i,j-1,k} - C_{ijk}) + {}^{t}w_{\mathrm{s}}(C_{i,j+1,k} - C_{ijk}) \\
& + {}^{t}w_{\mathrm{e}}(C_{i+1,j,k} - C_{ijk}) + {}^{t}w_{\mathrm{w}}(C_{i-1,j,k} - C_{ijk})] \\
& + \omega_{\mathrm{b}}[{}^{t}w_{\mathrm{ne}}(C_{i+1,j-1,k} - C_{ijk}) + {}^{t}w_{\mathrm{nw}}(C_{i-1,j-1,k} \\
& - C_{ijk}) + w_{\mathrm{se}}(C_{i+1,j+1,k} - C_{ijk}) \\
& + {}^{t}w_{\mathrm{sw}}(C_{i-1,j+1,k} - C_{ijk})] \qquad (25)
\end{aligned}
$$

where the terms ${}^{t}w_{\mathrm{n}}$, ${}^{t}w_{\mathrm{s}}$, ${}^{t}w_{\mathrm{e}}$, ${}^{t}w_{\mathrm{w}}$, ${}^{t}w_{\mathrm{ne}}$, ${}^{t}w_{\mathrm{nw}}$, ${}^{t}w_{\mathrm{se}}$, and ${}^{t}w_{\mathrm{sw}}$ indicate the magnitudes of wind velocity at the preceding time t in the north, south, east, west, north-east, north-west, south-east and south-west directions, respectively.

4.1.1.2. Turbulent diffusion. The impact of turbulence upon the concentration of the toxic material in a given cell *ijk* must also be considered; even more so in the case of dense gases. In the present model, the extent of vertical diffusion is characterized by the vertical entrainment velocity w_{e}, which is the effective velocity with which the ambient air becomes part of the plume. The vertical entrainment velocity is a function of the modified friction velocity, u_{T} and the plume Richardson number, Ri^{*} [67,68]. The modified friction velocity takes into account the impact of the underlying terrain upon the diffusion phenomenon. The modified friction velocity (u_{T}) may be represented in the following form [69]:

$$u_{\mathrm{T}} = [u_{*}^{2} + (aw_{*})^{2}]^{1/2} \quad \text{with} \quad a = 0.2 \qquad (26)$$

In the above expression, u_{*} is a fundamental scaling velocity called surface friction velocity which relates to the wind stress or drag generated as the wind travels through rough surfaces. It is measured as the square root of the surface stress, τ_0 divided by the air density, ρ_{a}. The friction velocity may be estimated as follows:

$$u_{*} = \frac{u}{(1/\kappa)\,\ln[(z-d)/z_0]} \qquad (27)$$

where u is the mean wind speed, κ the von Karman constant, z the height, d the displacement length which is a scaling length for describing wind profile at elevations close to average roughness obstacle height, and z_0 is the surface roughness length which is the measure of the amount of mechanical mixing introduced by the surface roughness elements. Typically, the values of u_{*} range from about 0.05 m/s in light winds to about 1 m/s in strong winds [70]. The term w_{*} is the convective velocity, i.e. the velocity of air entrainment as a result of the temperature difference between the substrate and the gas cloud. In an urban environment, local thermal sources are generated from energy stored in buildings from solar radiations or the direct heat generated from within the buildings or industrial plants and they constitute a source of turbulent kinetic energy within the obstacle array. This is in addition to the mechanically generated turbulence. The convective velocity may be estimated as:

$$w_{*} = \left(\frac{gH_{\mathrm{s}}H_{\mathrm{r}}}{\rho c_p T}\right) \qquad (28)$$

where g is the acceleration due to gravity, ρ, c_p and T the density, specific heat and temperature of the ambient air, H_{s} the heat generation or the release rate divided by the site area, and H_{r} is the average obstacle height. The plume Richardson number quantifies the intensity of denser-than-air-effects and is given by:

$$Ri^{*} = g\frac{(\rho_{\mathrm{p}} - \rho_{\mathrm{a}})h}{\rho_{\mathrm{a}}u_{*}} \qquad (29)$$

where g is the acceleration due to gravity, h the local cloud depth, ρ_{p} the initial density of the flammable gas cloud formed in the atmosphere, and ρ_{a} is the ambient air density. The expression for vertical entrainment velocity w_{e} [67] is given as follows:

$$w_{\mathrm{e}} = \frac{au_{\mathrm{T}}}{1 + b(Ri^{*})^{c}} \qquad (30)$$

where a, b, and c are the empirical constants. The value of a ranges between 0.4 and 0.8, b has an order of 1.0, and the value of c ranges from 0.5 to 1.0 [67,71–73]. The contributions of turbulent diffusion in the vertical direction may be incorporated in equation as follows:

$${}^{t+1}C_{ijk}^{\mathrm{tur}} = [k_z'(C_{i,j,k-1} - C_{ijk}) + k_z''(C_{i,j,k+1} - C_{ijk})] \qquad (31)$$

where k_z' and k_z'' are the components of the turbulent diffusivity constant k_z in the two cells in the vertical plane and are functions of the vertical entrainment velocity w_{e}. In the present model, we have considered k_z as follows:

$$k_z \propto (1 + \beta w_{\mathrm{e}}^{\gamma}) \qquad (32)$$

where β and γ are the empirical constants to be calibrated from experimental data. Thus, in the above expression, in the case when there is no turbulent diffusion at all, eddy diffusion coefficient coincides with the molecular diffusion coefficient. Taking Eq. (32) into consideration, we can rewrite Eq. (31) as follows:

$$
\begin{aligned}
{}^{t+1}C_{ijk}^{\mathrm{tur}} = {} & \omega_{\mathrm{a}}[(1 + \beta(w_{\mathrm{e}_{i,j,k-1}})^{\gamma})(C_{i,j,k-1} - C_{ijk}) \\
& + (1 + \beta(w_{\mathrm{e}_{i,j,k+1}})^{\gamma})(C_{i,j,k+1} - C_{ijk})] \qquad (33)
\end{aligned}
$$

Thus, adding the turbulent diffusion term to Eq. (25) we can again rewrite the expression for pollutant concentration in the cell *ijk* as follows:

$$
\begin{aligned}
{}^{t+1}C_{ijk} = {} & \omega_{\mathrm{a}}[{}^{t}w_{\mathrm{n}}(C_{i,j-1,k} - C_{ijk}) + {}^{t}w_{\mathrm{s}}(C_{i,j+1,k} - C_{ijk}) \\
& + {}^{t}w_{\mathrm{e}}(C_{i+1,j,k} - C_{ijk}) + {}^{t}w_{\mathrm{w}}(C_{i-1,j,k} - C_{ijk})] \\
& + \omega_{\mathrm{b}}[{}^{t}w_{\mathrm{ne}}(C_{i+1,j-1,k} - C_{ijk}) + {}^{t}w_{\mathrm{nw}}(C_{i-1,j-1,k} \\
& - C_{ijk}) + w_{\mathrm{se}}(C_{i+1,j+1,k} - C_{ijk}) + {}^{t}w_{\mathrm{sw}}(C_{i-1,j+1,k} \\
& - C_{ijk})] + \omega_{\mathrm{a}}[(1 + \beta(w_{\mathrm{e}_{i,j,k-1}})^{\gamma})(C_{i,j,k-1} - C_{ijk}) \\
& + (1 + \beta(w_{\mathrm{e}_{i,j,k+1}})^{\gamma})(C_{i,j,k+1} - C_{ijk})] \qquad (34)
\end{aligned}
$$

4.1.1.3. Transformation and deposition rate. Atmospheric processes such as chemical transformation and deposition may cause local level changes in the concentration of the toxic substance actually encountered by the receptors. The extent

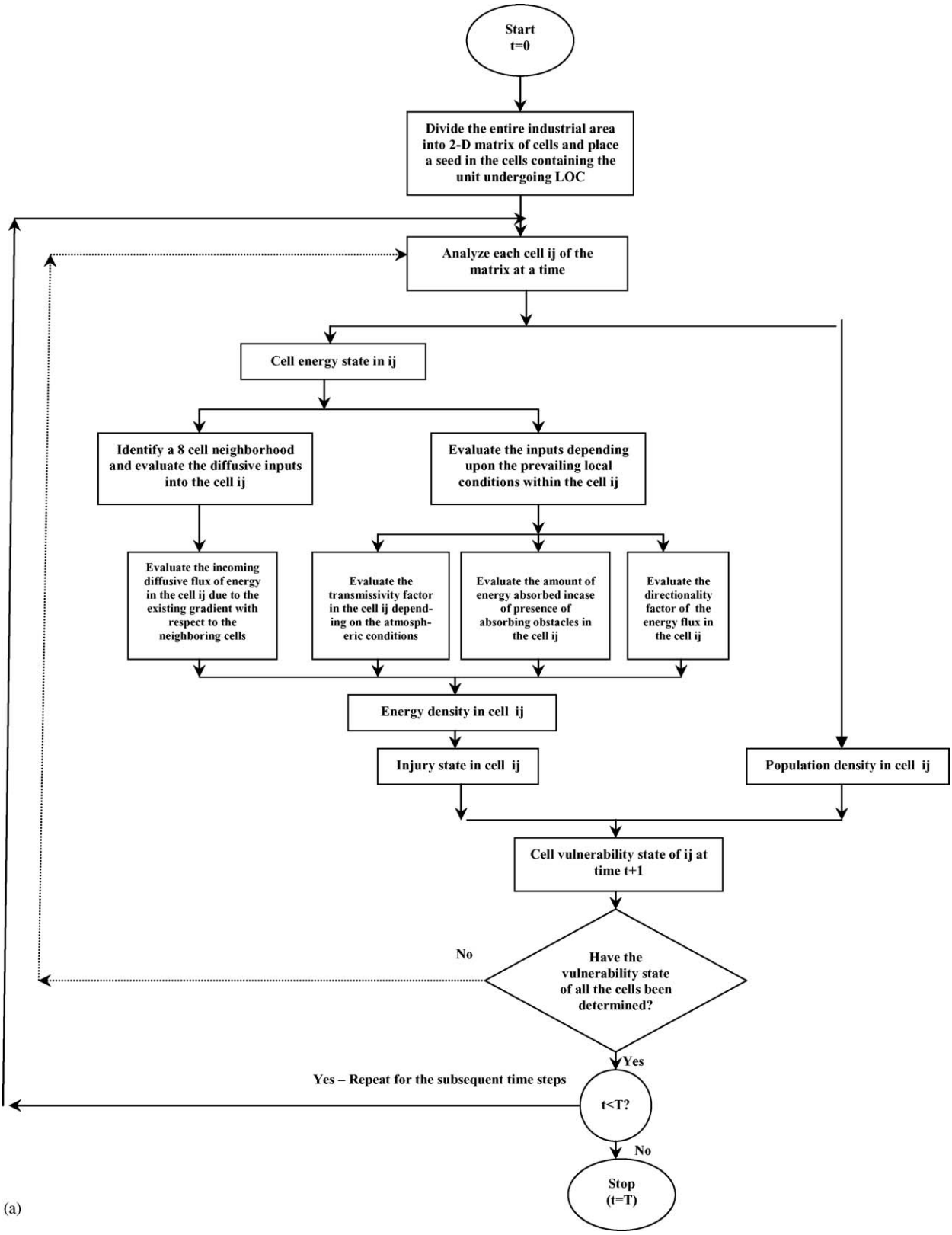

Fig. 5. (a) Algorithm for the modeling of flux of energy liberated from the unit suffering LOC with the help of CA approach; (b) algorithm for the modeling of flux of toxic material liberated from the unit suffering LOC with the help of CA approach.

Fig. 5. (*Continued*).

of these processes would depend upon the local atmospheric conditions prevailing in the cell *ijk* at time *t*. We have incorporated the impact of these processes in the model by taking into account the local transformation reaction or decay rate and the deposition rate of the released material in the cell *ijk*. Thus the overall toxicity state of a cell may be represented as:

$$
\begin{aligned}
{}^{t+1}C_{ijk} = {} & \omega_{\mathrm{a}}\left[{}^{t}w_{\mathrm{n}}(C_{i,j-1,k} - C_{ijk}) + {}^{t}w_{\mathrm{s}}(C_{i,j+1,k} - C_{ijk})\right. \\
& \left. + {}^{t}w_{\mathrm{e}}(C_{i+1,j,k} - C_{ijk}) + {}^{t}w_{\mathrm{w}}(C_{i-1,j,k} - C_{ijk})\right] \\
& + \omega_{\mathrm{b}}[{}^{t}w_{\mathrm{ne}}(C_{i+1,j-1,k} - C_{ijk}) + {}^{t}w_{\mathrm{nw}}(C_{i-1,j-1,k} \\
& - C_{ijk}) + w_{\mathrm{se}}(C_{i+1,j+1,k} - C_{ijk}) + {}^{t}w_{\mathrm{sw}}(C_{i-1,j+1,k} \\
& - C_{\mathrm{ijk}})] + \omega_{\mathrm{a}}[(1 + \beta(w_{\mathrm{e}_{i,j,k-1}})^{\gamma})(C_{i,j,k-1} - C_{ijk}) \\
& + (1 + \beta(w_{\mathrm{e}_{i,j,k+1}})^{\gamma})(C_{i,j,k+1} - C_{ijk})] \\
& - {}^{t}\delta_{ijk}{}^{t}C_{ijk} - {}^{t}\lambda_{ijk}{}^{t}C_{ijk} \qquad (35)
\end{aligned}
$$

4.1.2. Cell population state

As in the model for energy propagation discussed earlier, the cell population state P_{ijk} has been expressed in terms of the population density of any cell *ijk* at the time *t*.

4.1.3. Cell injury state

Similar to the concept employed in the CA model proposed for studying the energy propagation, the injury state of the cell *ijk* gives the probability of damage p_{ijk} which provides an indication of the extent of injury caused to the receptors as a result of the toxic concentration in that cell. It is a function of the magnitude of the flux of toxic material in the cell as well as the duration of exposure, i.e. the magnitude of each time step. It may be expressed as:

$$
{}^{t+1}\mathrm{In}_{C_{ijk}} = {}^{t+1}p_{C_{ijk}} = f({}^{t+1}\Phi_{C_{ijk}}, \Delta t) \qquad (36)
$$

where $p_{C_{ijk}}$ is the probability of damage due to toxic flux ${}^{t+1}\Phi_{C_{ijk}}$ reaching the cell *ijk* at time $t+1$ and Δt is the length of each time step. The overall vulnerability state of the cell *ijk*, ${}^{t+1}V_{ij}$ with respect to the toxic discharge accompanying the LOC in time $t+1$ may be expressed as:

$$
{}^{t+1}V_{ijk} = ({}^{t+1}P_{ijk} \times {}^{t+1}p_{C_{ijk}}) \qquad (37)
$$

5. Algorithms for modeling the propagation of the energy flux and the toxic material liberated due to LOC of a unit

Algorithms for modeling the propagation of energy and material due to the LOC of an industrial unit have been devel-

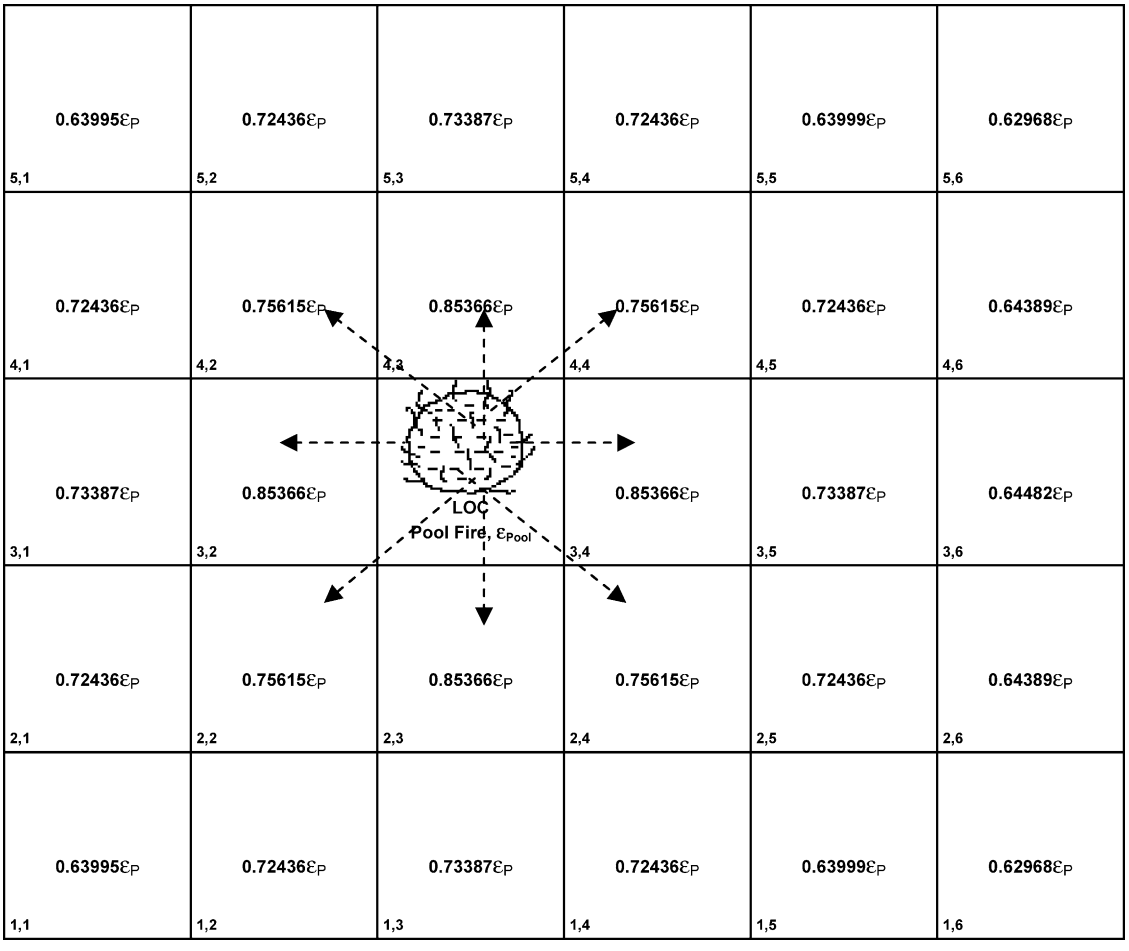

Fig. 6. Pattern of energy allocation for case 1.

oped by us, on the basis of the previously discussed models (Fig. 5). In the algorithm for propagation of energy, the study area has been notionally divided in to a 2D lattice of cells. The time has also been designated to proceed in equally spaced discrete intervals t, $t+1$, $t+2$, ..., T; where T is the user defined maximum limit of time for which the simulation is performed.

The simulation within the cellular automata paradigm is initiated from the cell containing the driving forces that govern the subsequent sequence of events. In the CA parlance, such cells are often called as 'seed cells' and the process of designating a seed cell is called 'placing a seed in the cell'. In the proposed model, the seed cell contains the unit that undergoes LOC. The simulation is initiated at the time $t=0$, which is the instant the unit in the seed cell undergoes LOC. The algorithm evaluates the energy state of each cell in the matrix by determining the magnitude of the energy gradient with respect to the neighbouring cells, taking into account the atmospheric transmissivity, the absorbtivities of the intercepting objects that may be present in the cell as well as the directionality of propagation of the energy flux.

In the case of dispersion of toxic material which has been treated as a three-dimensional phenomenon, the modeling algorithm is depicted in Fig. 5b. Here, the study area has been notionally divided in to a 3D lattice of cells. The rest of the sequence is almost similar to the energy propagation algorithm. During the emission of toxic material accompanying the LOC of a process unit, the ground level concentration allocated to each cell is evaluated by considering the inputs from the neighbouring cells due to advection and turbulent diffusion processes as well as calculating the rates of chemical transformation and sedimentation processes, which of course, depend on the prevailing local conditions of the cell.

The algorithm is run synchronously for each and every cell present in the lattice encompassing the study area. The emerging scenario in the subsequent time step is automated. The algorithm is run repeatedly in order to generate the scenarios for all subsequent time steps ($t+1, t+2, t+3\cdots\cdots\cdots+t+n$). This is pursued until the number of time steps becomes larger than the preset user-defined constant. Consequently, the algorithm is able to generate the corresponding vulnerability states of all the cells encompassing the study area at the end of every time step for which the simulations are performed.

It must be mentioned that approaches other than CA do exist in which attempts have been made to discretize the space through which the gas plume moves and to assess the role of each space (and time) element. Most noteworthy are the approaches using computational fluid dynamics (CFD). The numerical algorithm

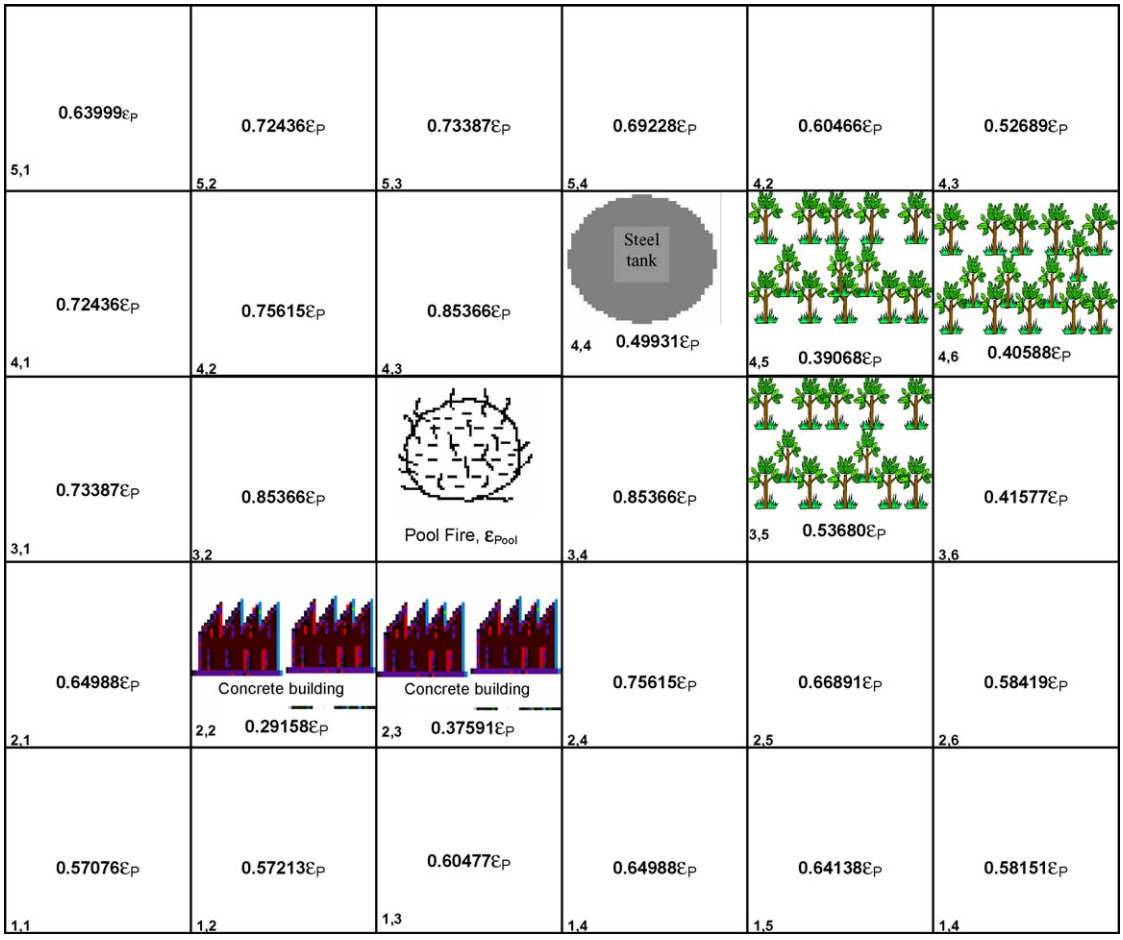

Fig. 7. Pattern of energy allocation for case 2.

in CFD utilize the utilize the finite differences and finite elements methods for performing numerical integration of the governing hydrodynamic equations. Generally, the partial differential equations whose independent variables are space and time are transformed into the mold of discrete space and time and numeric integration is performed by truncating the resulting power series to arrive at the corresponding *finite difference equations*, thereby replacing the continuous space and time into discrete grids. Nevertheless, significant errors are introduced in all such numerical simulations, since only a limited number of terms in the Taylor's series expansion are taken into account. The Navier–Stokes equation has long been employed to study the dynamics of atmospheric dispersion, but even the fastest computers have not been successful in solving these equations for fluid turbulence. Fluid turbulence has remained an unsolved problem on account of the large range of scales over which a solution must be applicable [74].

6. An illustrative example of the model application

We illustrate the application of the model with the help of the following hypothetical example:

- Site: a storage area of a petrochemical industry, with a dense network of supply pipelines.
- Scenario: a leak in one of the gasoline pipeline resulting in the formation of a liquid pool.
- Event: flashing of the leaked liquid propylene resulting in a pool fire.
- Study area: 0.3 ha divided into 2D lattice of 10 m × 10 m cells.
- Diameter of the liquid pool: 5.0 m.
- Heat radiated by the gasoline pool fire (E_p): 14244.5 KW.

The corresponding energy states of the each cell of the cellular matrix enveloping the study area have been evaluated for the three likely scenarios as follows:

- Case 1: Homogeneous environmental conditions
  - There exists no intercepting objects in any of the cells and all the cells have uniform (homogeneous) conditions.
  - The atmospheric transmissivity corresponds to 50% humidity throughout the entire cell matrix.
  - The directionality factor is negligible.

The simulation leads to energy allocation as depicted in Fig. 6.

- Case 2: Heterogeneous environmental conditions
  - Intercepting objects in the form of concrete building with an absorbtivity $\alpha \approx 0.73$ is present in the cells (2,2) and (2,3). An empty spherical steel tank with an absorbtivity of 0.39 is housed in the cell (4,4). While woody canopy with

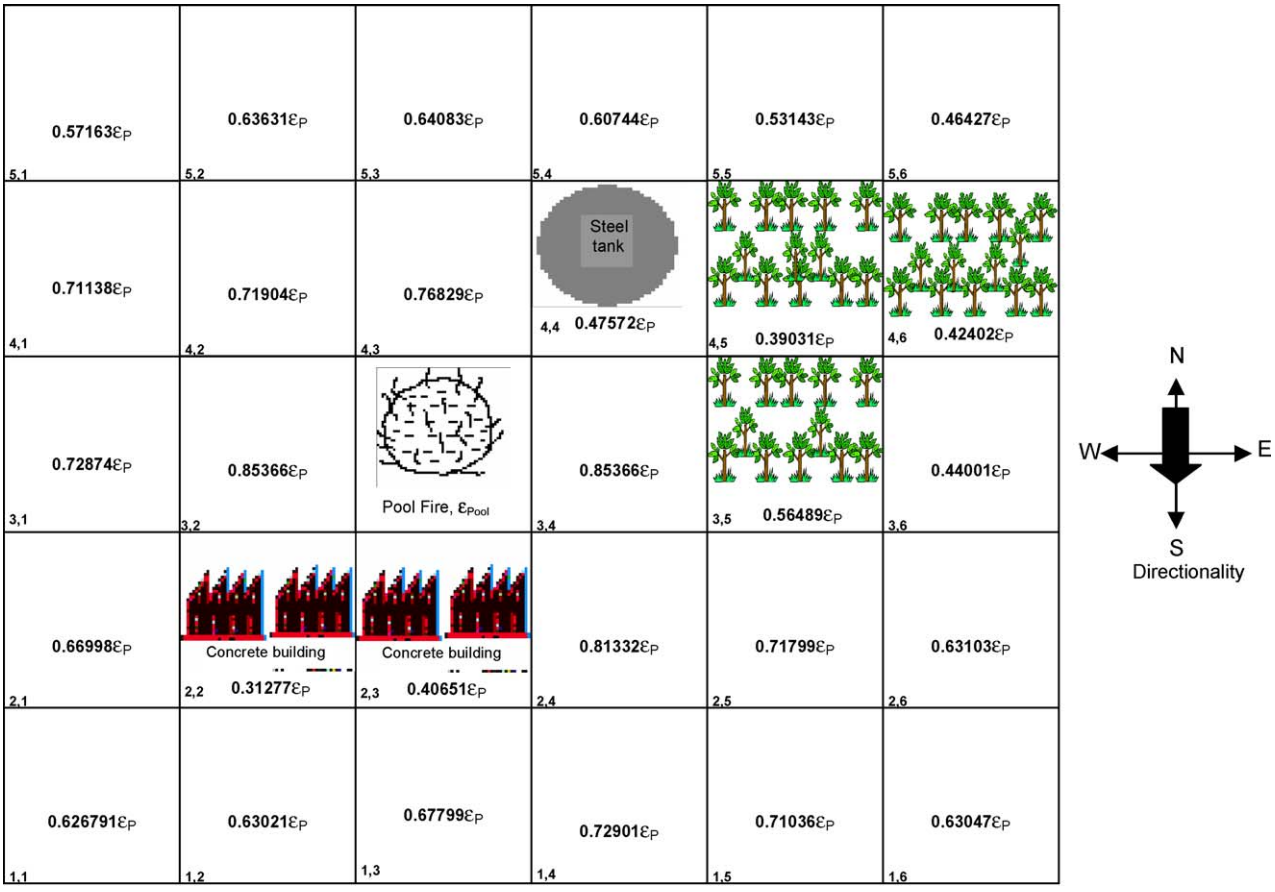

Fig. 8. Pattern of energy allocation for case 3.

has an absorbtivity $\alpha \approx 0.47$ happen to lie in the cells (3,5), (4,5), and (4,6).
- The atmospheric transmissivity is based on atmospheric humidity of 50% throughout the cellular matrix except in the cells (3,5), (4,5) and (4,6). Due to the presence of vegetation canopy in the cells (3,5), (4,5) and (4,6), the humidity is assigned to be 80% and the atmospheric transmissivity has been evaluated accordingly.
- The directionality factor is negligible.

The simulation leads to energy allocation in various cells as depicted in Fig. 7.

- Case 3: Heterogeneous environmental conditions with a specific directionality of propagation of the energy flux
  - Intercepting objects lie in the cells (2,2), (2,3), (4,4), (3,5), (4,5), and (4,6) as in case 2.
  - The atmospheric transmissivity is as in case 2.
  - The directionality of the energy flux is oriented along the southerly direction. The directional constants have been assigned the following values: ${}^{t}n_{ij} = -0.10$; ${}^{t}s_{ij} = +0.10$, ${}^{t}e_{ij} = {}^{t}w_{ij} = 0.0$, ${}^{t}ne_{ij} = {}^{t}nw_{ij} = -0.025$, ${}^{t}se_{ij} = {}^{t}sw_{ij} = +0.025$.

The pattern of energy allocation in the various cells obtained by simulation, is depicted in Fig. 8.

The energy states of each cell of the matrix enveloping the study area at the time step $t+1$ is represented in Figs. 6–8 illustrate. A comparison of the energy states of the various cells under the three scenarios is given in Table 1. It may be seen that the cell states in the three cases are different from each other, indicating that the flux of radiant energy released due to the LOC of the unit not only interacts with the prevailing local conditions (atmospheric transmissivity, absorbtivity of the intercepting objects located in the cell, directionality of propagation of the flux, etc.) but is also modified as a result of it during the course of its outward propagation. Consequently, the proposed model is able to identify the zones of impact and the degree of vulnerability posed to the receptors present in the zones.

A common pattern characterizing the self – evolution of all accidental events involves: an initial unsteady phase, a steady state wherein equilibrium is achieved, and finally a die down phase in which the intensity of the accidental event dissipates to zero. In most accidental events the three states are passed through very quickly. Irrespective of the duration of the accidental event, the mass and energy flux ensuing from the LOC, hence the toxicity and energy states of the cells, vary with time

Table 1
Comparison of the energy states of the various cells corresponding to the three cases

Cell coordinates	Radius perimeter (r)	Cell energy states at the time $t+1$ (kW)		
		Case 1	Case 2	Case 3
^{LOC}Cell 3,3	0	1.42444736E+4	1.42444736E+4	1.42444736E+4
Cell 2,2	1	1.07710726E+4	0.41534036E+4	0.44552639E+4
Cell 2,3		1.21599373E+4	0.53546543E+4	0.57904924E+4
Cell 2,4		1.07710726E+4	1.07710726E+4	1.15853010E+4
Cell 3,4		1.21599373E+4	1.21599373E+4	1.21599373E+4
Cell 4,4		1.07710726E+4	0.71124508E+4	0.67763097E+4
Cell 4,3		1.21599373E+4	1.21599373E+4	1.09439436E+4
Cell 4,2		1.07710726E+4	1.07710726E+4	1.02422836E+4
Cell 3,2		1.21599373E+4	1.21599373E+4	1.21599373E+4
Cell 1,1	2	0.91157508E+4	0.81302327E+4	0.89282366E+4
Cell 1,2		1.03182123E+4	0.81497619E+4	0.89769527E+4
Cell 1,3		1.04536203E+4	0.86147300E+4	0.96576106E+4
Cell 1,4		1.03182123E+4	0.92573124E+4	1.03843921E+4
Cell 1,5		0.91157508E+4	0.91361347E+4	1.01187612E+4
Cell 2,5		1.03182123E+4	0.95282907E+4	1.02275178E+4
Cell 3,5		1.04536203E+4	0.76464761E+4	0.80466461E+4
Cell 4,5		1.03182123E+4	0.55650850E+4	0.55597747E+4
Cell 5,5		0.91157508E+4	0.86131203E+4	0.75698836E+4
Cell 5,4		1.03182123E+4	0.98611641E+4	0.86526203E+4
Cell 5,3		1.04536203E+4	1.04536203E+4	0.91281663E+4
Cell 5,2		1.03182123E+4	1.03182123E+4	0.90639579E+4
Cell 5,1		0.91157508E+4	0.91157508E+4	0.81424972E+4
Cell 4,1		1.03182123E+4	1.03182123E+4	1.01332421E+4
Cell 3,1		1.04536203E+4	1.04536203E+4	1.03804464E+4
Cell 2,1		1.03182123E+4	0.92573053E+4	0.95435694E+4
Cell 1,6	3	0.89695028E+4	0.82833323E+4	0.89807560E+4
Cell 2,6		0.91676577E+4	0.83215502E+4	0.89887329E+4
Cell 3,6		0.91851214E+4	0.59224675E+4	0.62677678E+4
Cell 4,6		0.91676577E+4	0.57816794E+4	0.60399787E+4
Cell 5,6		0.89695028E+4	0.75052835E+4	0.66133002E+4

during the course of the accidental event. Pool fire, too, goes through changes in its form [2,13]. There is an initial induction phase when the burning rate accelerates as the increasing intensity of heat radiation increases the rate of evaporation of the liquid from the pool. A steady state is then achieved, followed by the non-equilibrium phase of gradual fire die down. The liquid burning rate, and hence, the amount of heat liberated from the pool fire is also influenced by factors such as pool diameter, flame lip effects, wind speed, etc. Accordingly, the cell will have different energy states at different time steps during the evolution of the pool fire depending upon the above-mentioned factors, besides, of course, the quantum of fuel involved in the pool fire and the prevailing ambient conditions at that time. The proposed model is capable of generating a 'cellular vulnerability mosaic' at the end of each time step to indicate the pattern of risk associated with the portion of the site enveloped by each cell.

The vulnerability of the surroundings to damage due to heat load emanated from an accidental fire at any particular time step, $t+n$, can be suitably represented with the help of the risk contours. As elaborated earlier, the conventional approach involves generation of contours in the form of concentric circles indicating the ranges of impacts such as zones of 100%, 75%, and 50% probability of burns [1,13,16] (Fig. 9a). However, the model now proposed by us is able to account for the heterogeneity in the area surrounding the jeopardized unit and the zones of impact are now forecast with much greater accuracy as is illustrated in Fig. 9b. It indicates that there will be a significant reduction in the magnitude of risk in the directions north and north-west to the unit suffering LOC in comparison to some other directions, owing to the presence of a concrete wall and forest which would absorb a fraction of the energy liberated from the LOC. There is also a perceivable reduction in the risk along the southern and southeasterly direction of the unit suffering LOC due to the presence of a wetland. From the Fig. 9a and b, it may be deduced that while the damage radii estimate of the conventional approach envelops the three cylindrical chemical storage tanks located north-west to the unit suffering LOC, the CA based estimate of the damage radii leaves them out. This is on account of the absorption of the incident energy flux by the concrete wall as well as the vegetation located north west of the unit suffering LOC.

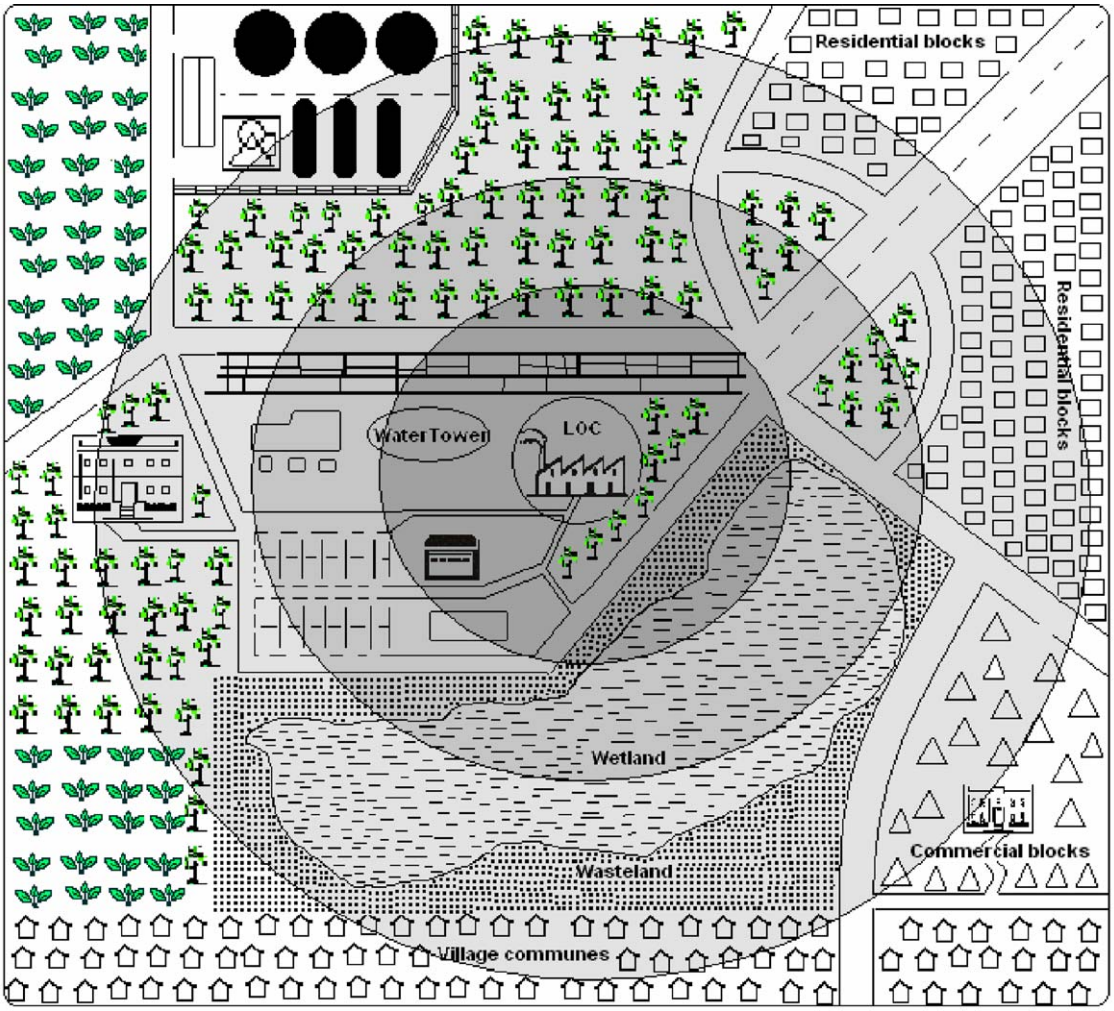

Fig. 9. (a) Vulnerability map indicating the impact range at time step $t+1$ obtained by the conventional approach; (b) vulnerability map indicating the risk contours at the time step $t+\Delta t$ obtained by the application of cellular automata approach.

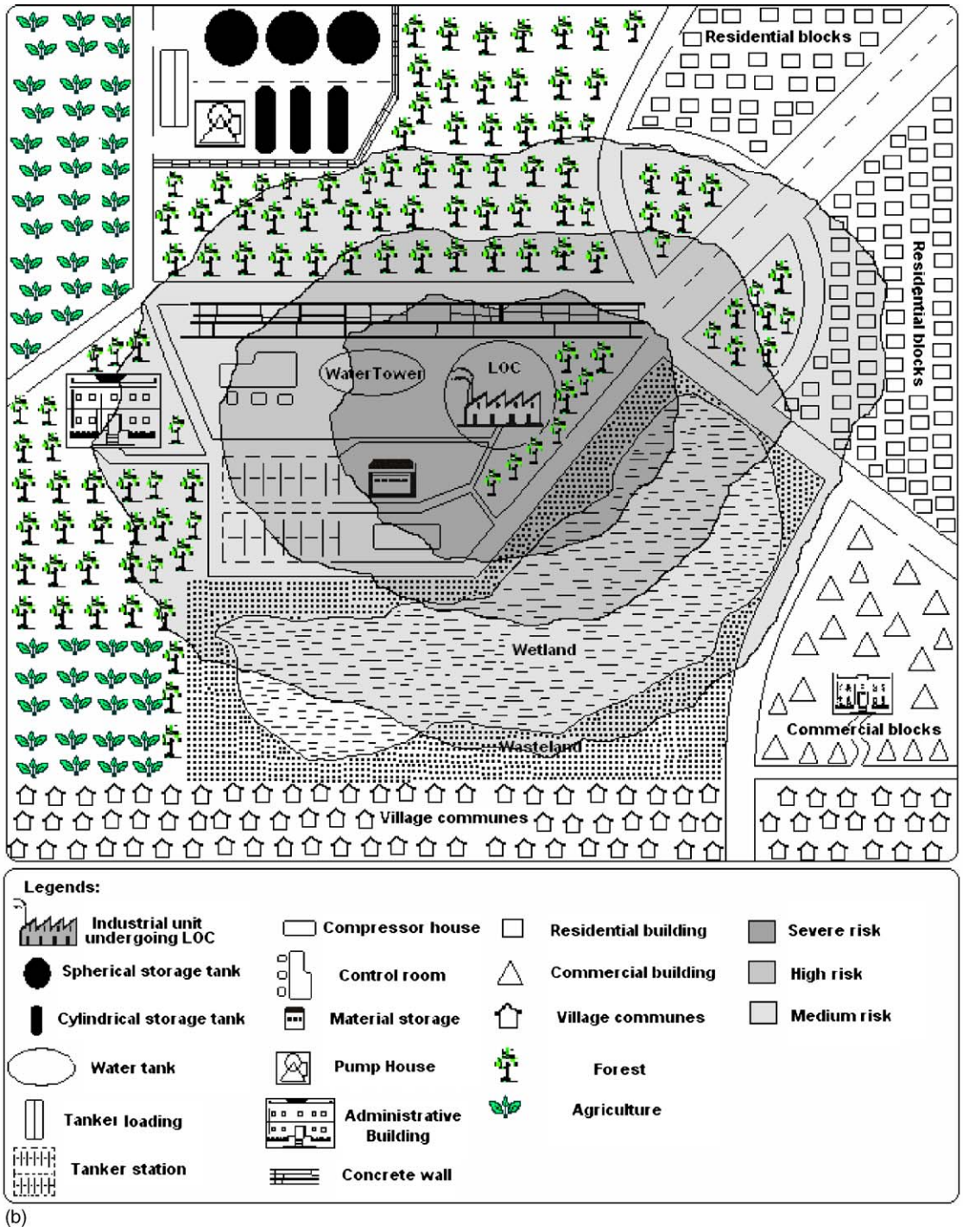

(b)

Fig. 9. (*Continued*).

7. Summary and conclusion

(a) The introductory part of the paper highlights the importance of accident scenario development as a common and crucial input to all methodologies dealing with the accident forecasting and loss prevention. It is, therefore, of utmost importance that techniques and methodologies are developed with which the impact of any likely accident at any given site is forecast with as great accuracy as possible.

(b) The state of the art is then briefly reviewed underscoring the need to develop methodologies for forecasting accident impacts which are able to account for the various objects (buildings, trees, other units, etc.) and environmental conditions (wind speed, wind direction, humidity, etc.) which typically exist at most accident sites and which lie in a heterogeneous, unsymmetrical manner around the accident epicentre. In the conventional methodologies, the accidental impact of fire and explosion is assumed to be propagating

outwards from the accidental epicenter in a radially symmetrical fashion; the only exception being the treatment of jet fire. With this basic assumption, the areas of impact of the accidents are denoted with circles. The areas corresponding to, say, 100%, 50%, 25% probability of death due to an accident are bounded by circles of increasing radii, with the accident site serving as the centre of the circles. In a similar fashion zones of impact are bounded for different probabilities of damage in other manner – for example eardrum rupture, burns, damage to structures, etc. Only when dealing with the accidental jet fire or the release of hazardous gases or liquids the areas of impact are computed on the basis of likely direction of the fire jet or the toxic plume movement. The later, in turn, is predicted on the basis of airshed/watershed characteristics of the accident site, and the 'roughness' of the terrain. But even in these treatments, the aspects such as impact of different types of structures, trees, wetlands, grasslands, etc. are not considered in detail.

(c) The fact is, in real-life situations, the conditions prevailing in the neighbourhood of the accident epicenter are rarely homogeneous. At the instant of time when the accident occurs, this heterogeneity of the neighbourhood strongly influences the outward propagation of not only the mass, but also energy and momentum away from the accident epicentre. Consequently, the area-of-impact of an accident would not be radially symmetrical, as is projected in conventional treatments of area-of-impact, but shall have an irregular shape.

(d) A methodology for accident modeling has been introduced, based on cellular automata. The movement of mass and energy which results from the accidental loss of confinement is modeled as a self-evolving phenomena occurring in discrete steps of space and time. It is considered that the types of objects and the meteorological conditions in each space element would influence this movement, either attenuating or exacerbating the mass/energy flux. This influence is accounted for in the model, resulting in much more realistic assessment of the 'zone of impact' of each accident. Consequently the damage potential of a likely accident is forecast with much greater accuracy. This treatment also enables an assessment of the 'diurnal variations' in risk – in other words the hour-to-hour variations in risk posed by the unit across each day–night cycle as a function of the number of people likely to be present at different times within the zone of impact, diurnal fluctuations in the area's micrometeorology, etc.Two specific CA-based models have been proposed for studying the nature of propagation of energy and toxic material emanated from the accident epicenter into the surroundings and thereby assessing the vulnerability posed to the potential receptors. The efficacy of the proposed models stems from the fact that in the CA-based discrete approach, one is able to take into account the influence of the site-specific factors associated with each area (grid) and thereby provide a credible simulation of the overall self evolution of the accidental scenario. The potential application of proposed models for risk estimation has been illustrated with a case study dealing with the propagation of heat load from a pool fire.

(e) It must be emphasized that cellular automaton is a computational tool, the effectiveness of which depends upon its accurate calibration on the basis of data from experimental observations as well as those from past accident histories. Research in these areas has been continuing across the world but needs greater impetus.

(f) Future research may also be directed towards optimized identification of the seed cell for effective scenario generation with CA. The CA-based approach described herein attempts to simulate a point source phenomenon and the seed cell is the one where the initiating event terminating into the uncontrolled transfer of energy, mass and momentum, is localized. For studying the behaviour of spatially distributed phenomenon such as a vapour cloud explosion, fireball, etc., careful consideration must be given to the choice of the exact location of seed cell. For example, vapour cloud explosion results from the ignition of a flammable cloud formed due to the LOC of a vessel containing flammable vapourizing liquid or gas. Rather than considering such a phenomenon as an entity, it is advantageous to consider a vapour cloud explosion to be comprising of a number of sub-explosions corresponding to the various sources of blast in the cloud as has been envisaged in multi-energy concept. In such a scenario, the seed cell must comprise of the volume where the cloud lies within the flammable range of the material and where the ignition actually occurs. Thus in this case the choice of the exact location of the seed cell is governed by the intrinsic characteristics of the cloud as well as an investigation of the prevailing environmental conditions on potential blast generative capabilities especially the degree of turbulence and the nature of obstructions within the cloud, in case of a partially confined gas cloud. Thereafter, overpressures generated as a result of the outward propagation of the flame in a turbulent medium may be simulated using the cellular automata approach. The flexibility in the choice of the seed cell is advantageous since it enables us to iterate among the various potential scenarios resulting from different events.

Acknowledgements

Authors thank the Department of Science and Technology, Government of India, New Delhi, for support under its Chemical Engineering Programme. Authors also thank the anonymous referees for their painstaking review and incisive comments which have greatly helped us in refining the paper.

References

[1] F.I. Khan, S.A. Abbasi, Techniques and methodologies for risk analysis in chemical process industries, J. Loss Prevent. Process Ind. 11 (4) (1998) 261–277.

[2] F.P. Lees, Loss Prevention in the Process Industries, 2nd ed., Butterwort-Heinemann, Oxford, UK, 1996.

[3] F.P. Lees, Lee's Loss Prevention in the Process Industries, 3rd ed., Butterwort-Heinemann, Oxford, U.K., 2005 (partially updated by S. Mannan).

[4] T. Abbasi, S.A. Abbasi, The expertise and the practice of loss prevention in India – pointers for the third world, Trans. IChemE: Process Safety Environ. Protect. 83-B5 (2005) 413–420.
[5] T.A. Kletz, Eliminating potential process hazard, Chem. Eng. 48 (1985).
[6] F.I. Khan, S.A. Abbasi, Accident Hazard Index: a multi-attribute method for process industry hazard rating, Trans. IChemE 75 (Part B) (1997) 217–224.
[7] F.I. Khan, S.A. Abbasi, OptHAZOP – an effective and optimum approach for HAZOP study, J. Loss Prevent. Process Ind. 10 (3) (1997) 191–204.
[8] F.I. Khan, S.A. Abbasi, Mathematical model for HAZOP study time estimation, J. Loss Prevent. Process Ind. 10 (4) (1997) 249–257.
[9] F.I. Khan, S.A. Abbasi, TOPHAZOP: a knowledge based software tool for conducting HAZOP in a rapid, efficient yet inexpensive manner, J. Loss Prevent. Process Ind. 10 (5–6) (1997) 333–343.
[10] F.I. Khan, S.A. Abbasi, A criterion for developing credible accident scenarios for risk assessment, J. Loss Prevent. Process Ind. 15 (2002) 467–475.
[11] F.I. Khan, S.A. Abbasi, Analytical simulation and PROFAT II: a new methodology and computer automated tool for fault tree analysis in chemical process industries, J. Hazard. Mater. A 75 (2000) 1–27.
[12] F.I. Khan, S.A. Abbasi, Risk Assessment in Chemical Process Industries: Advanced Techniques, Discovery Publishing House, New Delhi, 1998, ix+364 pages.
[13] Centre for Chemical Process Safety (CCPS) of the American Institute of Chemical Engineers, Guidelines for Chemical Process Quantitative Risk Analysis, 2nd ed., 2000.
[14] Committee for Prevention of Disasters caused by Dangerous Substances, Methods for determining possible damage to people and subjects from releases of hazardous materials – Green Book, 1st ed., 1992. CPR 16E.
[15] Committee for Prevention of Disasters, Methods for determining and processing probabilities – Red Book, 2nd ed., 1997. CPR 12E.
[16] Committee for Prevention of Disasters, Methods for calculating physical effects resulting from releases of hazardous materials – Yellow Book, 3rd ed., 1997. CPR 14E.
[17] Committee for Prevention of Disasters, Guidelines for quantitative risk assessment – Purple Book, 1st ed., 1999. CPR 18E.
[18] T. Abbasi, S.A. Abbasi, 2006. The boiling liquid expanding vapour explosion (BLEVE): mechanism, consequence assessment, management, J. Hazard. Mater., in press.
[19] F.I. Khan, P. Amyotte, Inherent safety in offshore oil and gas activities: a review of the present status and future directions, J. Loss Prevent. Process Ind. 15 (2002) 279–289.
[20] G. Vijayaraghavan, Impact assessment, modeling, and control of dust explosions in chemical process industries, M.Tech. Thesis, Department of Chemical Engineering, Coimbatore Institute of Technology, April, 2004.
[21] M. Batty, P.M. Torrens, Modeling and prediction in a complex world, Futures 37 (7) (2005) 745–766.
[22] Von Neumann J., 1966. Theory of Self-reproducing Automata, edited and completed by A Burks (University of Illinois Press, Urbana, IL).
[23] S. Ulam, Random processes and transformations, Proc. Int. Congr. Math. 2 (1952) 264–275.
[24] G.Y. Vichniac, Simulating physics with cellular automata, Physica D 10 (1984) 96–116.
[25] R.M. Itami, Simulating spatial dynamics: cellular automata theory, Landscape Urban Plan. 30 (1994) 27–47.
[26] E.F. Codd, Cellular Automata, Academic Press, 1968.
[27] C.G. Langton, Self reproduction in cellular automata, Physica D 10 (1984) 135–144.
[28] J. Byl, Self reproduction in cellular automata, Physica D 34 (1989) 259–299.
[29] M. Gardner, On cellular automata, self reproduction, the Garden of Eden and the game 'Life', Sci. Am. 224 (2) (1971) 112–117.
[30] D. Talia, P. Sloot, Cellular automata: promise and prospects in computational science, Future Gener. Comp. Syst. 16 (1999) v–vii.
[31] C.M. Herr, T. Kvan, Adapting cellular automata to support the architectural design process, Automat. Constr., in press (Corrected Proof, Available online 30 November 2005).
[32] Q. Chen, A.E. Mynett, Effects of cell size and configuration in cellular automata based prey–predator modelling, Simulat. Model. Practice Theory 11 (2003) 609–625.
[33] C. He, Q. Zhang, Y. Li, X. Li, P. Shi, Zoning grassland protection area using remote sensing and cellular automata modelling—A case study in Xilingol steppe grassland in northern China, J. Arid Environ. 63 (2005) 814–826.
[34] C. Bone, S. Dragicevic, Arthur Roberts, A fuzzy-constrained cellular automata model of forest insect infestations, Ecol. Model. 192 (1–2) (2006) 107–125.
[35] R. Willox, B. Grammaticos, A.S. Carstea, A. Ramani, Epidemic dynamics: discrete-time and cellular automaton models, Phys. A: Stat. Mech. Appl. 328 (1–2) (2003) 13–22.
[36] R.J. Doran, S.W. Laffan, Simulating the spatial dynamics of foot and mouth disease outbreaks in feral pigs and livestock in Queensland, Australia, using a susceptible-infected-recovered cellular automata model, Prev. Vet. Med. 70 (1–2) (2005) 133–152.
[37] G.M. Crisci, S. Di Gregorio, R. Rongo, W. Spataro, PYR: a cellular automata model for pyroclastic flows and application to the 1991 Mt. Pinatubo eruption, Future Gener. Comp. Syst. 21 (7) (2005) 1019–1032.
[38] G. Iovine, D. D'Ambrosio, S. Di Gregorio, Applying genetic algorithms for calibrating a hexagonal cellular automata model for the simulation of debris flows characterized by strong inertial effects, Geomorphology 66 (2005) 287–303.
[39] G.Ch. Sirakoulis, I. Karafyllidis, Ch. Mizas, V. Mardiris, A. Thanailakis, Ph. Tsalides, A cellular automaton model for the study of DNA sequence evolution, Comp. Biol. Med. 33 (2003) 439–453.
[40] J. Freudenberg, T. Schiemann, U. Tiede, K.H. Hohne, Simulation of cardiac excitation patterns in a three-dimensional anatomical heart atlas, Comp. Biol. Med. 30 (2000) 191–205.
[41] D.G. Mallet, L.G. De Pillis, A cellular automata model of tumor–immune system interactions, J. Theor. Biol. 239 (3) (2006) 334–350.
[42] S. Maerivoet, B. De Moor, Cellular automata models of road traffic, Phys. Rep. 419 (2005) 1–64.
[43] M.S. Watanabe, Dynamics of group motions controlled by signal processing: a cellular-automaton model and its applications, Commun. Nonlinear Sci. Numer. Simulat. 11 (2006) 624–634.
[44] F. Seredynski, P. Bouvry, A.Y. Zomaya, Cellular automata computations and secret key cryptography, Parallel Comput. 30 (2004) 753–766.
[45] L Rosin, Training cellular automata for image processing, in: H. Kalviainen, et al. (Eds.), Proceedings of the 14th Scandinavian Conference on Image Processing, LNCS 3540, Springer-Verlag, Berlin Heidelberg, 2005, pp. 195–204.
[46] A.D. Syphard, K.C. Clarke, Janet Franklin, Using a cellular automaton model to forecast the effects of urban growth on habitat pattern in southern California, Ecol. Complex. 2 (2) (2005) 185–203.
[47] S. Fang, G.Z. Gertner, Z. Sun, A.A. Anderson, The impact of interactions in spatial simulation of the dynamics of urban sprawl, Landscape Urban Plan. 73 (4) (2005) 294–306.
[48] C. Sarkar, S.A. Abbasi, Enhancing the accuracy of forecasting impact of accidents in chemical process industry by the application of cellular automata technique, Trans. IChemE: Part B. Process Safety Environ. Protect. 84 (B4) (2006) 1–16.
[49] S. Wolfram, Cellular automata as models of complexity, Nature 31 (4) (1984) 419–424.
[50] S. Wolfram, A New Kind of Science, Wolfram Media, Champaign, 2002.
[51] G. Faraco, P. Pantano, R. Servidio, The use of Cellular Automata in the learning of emergence, Comp. Educ., in press (Corrected Proof, Available online 8 December 2004).
[52] X. Li, A.G.O. Yeh, Calibration of cellular automata by using neural networks for the simulation of complex urban systems, Environ. Plan. A 33 (2001) 1445–1462.

[53] X. Li, A.G.O. Yeh, Neural-network-based cellular automata for simulating multiple land use changes using GIS, Int. J. Geogr. Inf. Sci. 16 (4) (2002) 323–343.
[54] I. Karafyllidis, Acceleration of cellular automata algorithms using genetic algorithms, Adv. Eng. Software 30 (1999) 419–437.
[55] I. Karafyllidis, Design of a dedicated parallel processor for the prediction of forest fire spreading using cellular automata and genetic algorithms, Eng. Appl. Artif. Intell. 17 (2004) 19–36.
[56] R.G. Pontius, J. Malanson, Comparison of the structure and accuracy of two land change models, Int. J. Geogr. Inf. Sci. 19 (2) (2005) 243–265.
[57] K. Clarke, S. Hoppen, L. Gaydos, Methods and techniques for rigorous calibration of cellular automaton model of urban growth, in: Proceedings of the 3rd International Conference/Workshop on Integrating GIS and Environmental Modeling, Santa Fe, New Mexico, 1996.
[58] K. Clarke, S. Hoppen, L. Gaydos, A self-modifying cellular automaton model of historical urbanization in the San Francisco Bay area, Environ. Plan. B: Plan. Design 24 (1997) 247–261.
[59] F. Wu, Simulating urban encroachment on rural land with fuzzy-logic-controlled cellular automata in a geographical information system, J. Environ. Manage. 53 (4) (1998) 293–308.
[60] Y. Liu, S.R. Phinn, Modeling urban development with cellular automata incorporating fuzzy-set approaches, Computers, Environ. Urban Syst. 27 (2003) 637–658.
[61] F. Wu, C.J. Webster, Simulation of land development through the integration of cellular automata and multi-criteria evaluation, Environ. Plan. B: Plan. Design 25 (1) (1998) 103–126.
[62] R. Siegel, J.R. Howell, Thermal Radiation Heat Transfer, McGraw-Hill Kogakusha Ltd., 1972.
[63] C.M. Pietersen, S.C. Huerta, Analysis of the LPG incident in San Juan Ixhuatepec, Mexico City, 19 Nov 1984. TNO84-0222. Netherlands Organization for Applied Scientific Research, Apeldoorn, The Netherlands, 1985.
[64] M.D. Christou, M. Matterelli, Land use planning in the vicinity of chemical sites: risk-informed decision making at a local community level, J. Hazard. Mater. 78 (2000) 191–222.
[65] K.W. Lee, A methodology for assessing risk for released hydrocarbon in an enclosed area, J. Loss Prevent. Process Ind. 15 (2002) 11–17.
[66] V. Cozzani, E. Salzano, The quantitative assessment of domino effects caused by overpressure. Part I. Probit models, J. Hazard. Mater. A 107 (2004) 67–80.
[67] S.R. Hanna, K.W. Steinberg, Overview of Petroleum Environment Research Forum (PERF) dense gas dispersion modeling project, Atmos. Environ. 35 (2001) 2223–2229.
[68] R.E. Britter, S.R. Hanna, G.A. Briggs, A. Robins, Short-range vertical dispersion from a ground level source in a turbulent boundary layer, Atmos. Environ. 37 (2003) 3885–3894.
[69] K.J. Eidsvik, A model for heavy gas dispersion in the atmosphere, Atmos. Environ. 14 (1980) 769–777.
[70] S.R. Hanna, R.E. Britter, Wind Flow and Vapor cloud Dispersion at Industrial and Urban Sites, Center for Chemical process Safety of the American Institute of Chemical Engineers, New York, 2002.
[71] J.A. Havens, T.O. Spicer, Development of an atmospheric dispersion model for heavier than air gas mixtures, Final Report to the US Coast Guard, CG-D-23-85, USCG HQ, Washington, DC, 1985.
[72] D.L. Ermak, User Manual for SLAB: An Atmospheric Dispersion Model for Denser-Than-Air-Releases, UCRL-MA-105607, Lawrence Livermore National Laboratory, Livermore, CA, 1990.
[73] H.W.M. Witlox, The HEGADAS model for ground-level heavy-gas dispersion. II. Time dependant model, Atmos. Environ. 28 (1994) 2933–2940.
[74] D.L. Turcotte, The relationship of fractals in geophysics to "the new science", Chaos, Solitons Fractals 19 (2) (2004) 255–258.